
Response to Hans-Werner Jacobi

Do the authors use the term “equivalent black carbon” as defined regarding atmospheric black carbon measurements (i.e. linked to aethalometer measurements) or do the authors imply that all absorbing impurities in the snow are represented by black carbon?

Until now, in the radiative model TARTES, all absorbing impurities are represented by black carbon. That’s why we use the term « equivalent black carbon ».

What are the simulated impurity concentrations in the snowpack? What are the calculated dry deposition fluxes? Do the concentrations and fluxes agree with what can be expected from observations? What atmospheric concentrations are required to maintain the assumed fluxes?

The dry and wet deposition fluxes are perturbed parameters of the ensemble. This is explained section 3.4 “Perturbation of impurity deposition rate”. The dry deposition flux varies from 0 to $0.5 \text{ ng g}^{-1} \text{ s}^{-1}$ with a median value is $0.015 \text{ ng g}^{-1} \text{ s}^{-1}$ in concentration which roughly corresponds to $3.5 \text{ kg m}^2 \text{ s}^{-1}$. This is the same order of magnitude than the dry deposition rates obtained for this location using ALADIN-Climat (Nabat et al., 2015) simulations.

The simulated impurity content varies a lot, for example fresh snow values varies from 0 to 500 ng g^{-1} BC equivalent with a median value of 100 ng g^{-1} . Measurement in the field performed at col de Porte on the 2014/02/11 on fresh snow shows a value of 20 ng g^{-1} BC equivalent at the surface. The evolution of impurity content in the simulated snowpack has to be investigated using more field measurements but this is not the main objective of the present study.

What is the basis for distributing the deposited impurities in the top 5 cm?

The exponential decay is used to mimic the dry deposition of impurity at the surface of the snow layer. The value of 5 cm was chosen almost arbitrarily. Changing this value (within a reasonable range) does not significantly impact the simulations.

Since the absorbing impurities can have a large impact on the albedo, can the MODIS data be used to constrain the parameters used for the deposition?

Yes definitely, the assimilation scheme can be used to provide updated value for deposition rates and that’s one of the thing we plan to do in future work.

The authors are very grateful for this in depth review of the paper. All the reviewer comments have been taken into account in the new version of the manuscript. This is described in the detailed response below each comment. Proposed changes in the new version of the manuscript are highlighted in bold.

ANONYMOUS REVIEWER, REVIEW 1

GENERAL COMMENTS

- I think the authors have conducted a valuable and interesting analysis. To my knowledge, the assimilation of reflectance data is novel and the authors demonstrate a clear benefit for this practice. They have established a basis for future work that may have a greater impact, including the use of real-time remote sensing data from MODIS and operational implementations. I think the paper should be published pending attention to a suite of minor revisions.

- The manuscript lacks substantive discussion of the results, and this is the main weakness of the study in my opinion. I think the authors need to place some attention on contextualizing their results, comparing their results to prior research, and anticipating future work.

We completely agree on this point and for that matter, we modified the introduction section, the section 5 “assimilation of MODIS-like reflectances” and also the section 6.4 “Combining reflectance and snow depth assimilation”.

All modifications are indicated here in bold.

Introduction

-----NEW-----

Seasonal snowpack modeling is a crucial issue for a large range of applications, including the forecast of natural hazards such as avalanches or floods, or the study of climate change (e.g. \citealp{durand1999,lehning2006,bavay2013}). The most sophisticated detailed snowpack models represent the evolution of snow microstructure and the layering of snow physical properties \citep{brun1989,brun1992,jordan1991,Bartelt2002,vionnet2012} in response to meteorological conditions. Despite constant efforts to improve these models, large uncertainties remain in the representation of the snow physics, as well as in the meteorological forcings \citep{carpenter2004,essery2013,raleigh2014}. These uncertainties are highly amplified when propagated to avalanche hazard models \citep{vernay2015}. For operational applications, the assimilation of observations can help reduce the impact of the model and forcing uncertainties in the snowpack simulations \citep[e.g.]{dechant2011}.

Satellite observations are becoming an essential component of snow modeling and forecasting systems.

\textit{In situ} measurements are the most detailed and accurate observations of the snowpack, but their spatial distribution is far too scarce to capture the high spatial variability of the seasonal snowpack properties and improve snowpack simulations through their assimilation. For this reason, the assimilation of satellite observations of snow is an active area of research.

Snow remote sensing is primarily performed in the microwave (passive and active), visible and near-infrared spectra. Since the direct assimilation of such data requires the use of radiative transfer models, a common and simple approach consists in using satellite-based snow products. In particular, the assimilation of snow cover fraction (SCF) estimates derived from optical sensors (such as MODIS) and Snow Water Equivalent (SWE) or Snow Depth (SD) estimates derived from passive microwave sensors (such as AMSR-E) has been investigated extensively \citep{sun2004, andreadis2006, clark2006, dong2007, de2012, liu2013}.

These studies have suggested that, most of the time, assimilating snow observations may be useful to improve snowpack estimation. SWE or SD assimilation generally outperforms the assimilation of SCF only, except from \citep{andreadis2006} because of large errors in the AMSR-E SWE products. The assimilation of both combined revealed larger benefit by mitigating sensors limitations. Recently, \citep{navari2015} investigated the assimilation of (synthetic) ice surface temperature while \citep{dumont2012} also experimented the assimilation of albedo retrievals, both from optical sensors. \citep{dumont2012} obtained a mass balance RMSE decrease of up to 40\% assimilating albedo data. However, satellite snow products are derived using retrieval algorithms which are not perfect and, perhaps more importantly, not physically consistent with the snowpack model used for the data assimilation. For this reason, and as advocated by \citep{durand2009} who tested the assimilation of in situ microwave radiance observations, assimilating the original satellite radiance data should be preferred when possible.

% Active microwave data

The potential of assimilating passive microwave radiances (in the form of brightness temperature) collected by AMSR-E satellite have been examined by \citep{dechant2011} and \citep{che2014}. Significant improvements in the SWE/SD predictions occurred but only during the accumulation period. Though the melt period, when the snowpack is wet, liquid water alters the microwave signal resulting in a lower performance of the assimilation. Moreover, for small-scale applications in mountainous areas, the coarse spatial resolution of these data considerably reduces their usefulness \citep{foster2005, cordisco2006, dong2007, tedesco2010}. As for active microwave measurements, several tests have been conducted to assimilate the satellite signal (e.g. \citealp{stankov2008, phan}). These tests were however limited by the accuracy of the forward electromagnetic models and by the current lack of satellite data at a daily or even weekly time frequency.

% VIS/NIR microwave data

Visible and near-infrared reflectances from satellite observations have never been assimilated into snowpack models despite their great sensitivity to the snowpack properties \citep{warren1982}. Even if cloud cover might limit their utility, medium and high spatial resolution data are available at daily resolution from several optical sensors (e.g. MODerate

resolution Imaging Spectrometer, Visible Infrared Imaging Radiometer Suite) and seem to be quite suitable for complex topography \cite{sirguey2009}. In particular, the MODIS sensor, onboard TERRA and AQUA satellites, offers a daily coverage and provides reflectance measurements in seven bands distributed in the visible (at 250 to 500 m spatial resolution), near and short-wave infrared wavelengths. Surface bi-hemispherical reflectances corrected from complex topographic effects in mountainous areas can be computed \cite{sirguey2009} and have been evaluated and used in several rugged areas \cite{dumont2012, brun2015}.

5. Assimilation of MODIS reflectances:

-----NEW-----

Figure \ref{RMSE_8009} shows the time evolution of the RMSE with assimilation at every observation time, at the end of the forecast step (blue solid line) and just after the filter analysis (blue dotted line). These results are compared to the RMSE without assimilation (grey lines). The RMSE of the ensemble with assimilation is always lower than the RMSE without assimilation. **Averaged over the season, a reduction of 46\% was obtained for SD and 44\% for SWE, (Table \ref{RMSE_result}: seasonal RMSE for SD: 0.07 m; SWE: 19.7 kg\,m⁻² compared to 0.13 m and 35.4 kg\,m⁻² from the ensemble without assimilation).** These results indicate the usefulness of using spectral optical radiance rather than albedo data since \cite{dumont2012} obtained an improvement in SD estimate of only 14\% when assimilating albedo retrievals from MODIS sensor. It is remarkable that, despite the significant RMSE reduction in our experiment, there is most of the time no strong reduction of the RMSE from a **single analysis**. The reduced RMSEs with assimilation are consequently due to the successive observations throughout the season, highlighting the role of model dynamics.

[...]

The remarks stated above for the season 2010/2011 hold for the other seasons. Figure \ref{RMSE_5seasons} reports the time evolution of the SD and SWE RMSEs for all the selected seasons, in the experiments without assimilation (red lines) and with assimilation of reflectances (blue line; the experiments shown in green and black are discussed in the next section). On average, SD and SWE RMSEs are reduced by 45\% and 48\%, respectively. This is comparable with results of \cite{che2014}, who assimilate radiances in the microwave spectrum from AMSR-E, and reduce the SD RMSE by 50\%. However, passive microwave observations are very sensitive to liquid water. Consequently, the performance of the assimilation during the melting period is reduced (\cite{che2014} reduce the SD RMSE up to 61\% from January to March, during only the dry snow period). In contrast, our results show a well-marked reduction of errors near the end of the seasons (Figure \ref{RMSE_result}, grey lines and blue dotted lines). Our results are also consistent with those from \cite{liu2013} assimilating MODIS-derived Snow Cover Fractions (SCF), after a processing of the retrieval to improve accuracy of cloud coverage and snow mapping. Without this processing, the performance of SCF assimilation falls, with a SWE RMSE reduction near 10-20\%, similarly to \cite{andreadis2006}.

6.4 Combining reflectances and snow depth assimilation

-----NEW-----

These results indicate the usefulness of combining these two datasets in operational applications. \cite{liu2013} reached a similar conclusion by combining the assimilation of SCF and SD (with an SWE RMSE reduction up to 72\%; up to 74\% in our study). However, given the strong spatial variability of the snow cover, the spatial representativity of punctual SD measurements may make their assimilation questionable. This issue should be addressed with experiments over two-dimensional, realistic domains.

- I think it would be beneficial for the authors to discuss what is necessary to include a radiative transfer model like TARTES in a snow model (instead of an albedo parameterization). This is important because it seems that the only way to assimilate remotely sensed reflectance into an existing model is to ensure that it has the capability of outputting reflectance data at different wavelengths. Many, if not most, existing snow models do not have this capacity. So it would be useful to have some discussion about the changes required in the model structure, runtime, and operation, and what level of complexity is needed in order to achieve the methodologies demonstrated with Crocus.

The section 2.3 has been modified accordingly.

Given that satellite observations indirectly relate to the quantities of interest, an observation operator is required to link the satellite observation and the model state variables \citep{reichle2008}. This operator transforms the model variables into diagnostic variables to allow a direct comparison with satellite observations, preserving the physical consistency of the satellite signal with the snow model.

To this end, a new radiative transfer model was recently implemented in Crocus to calculate spectral reflectances that can be used for the comparison and the assimilation of satellite data such as MODIS. This model, named TARTES (Two-streAm Radiative TransfEr in Snow, Libois et al., 2013, 2014), simulates the absorption of solar radiation within the stratified snowpack using the δ -Eddington approximation, with a spectral resolution of 20nm. This contrasts with the original version of Crocus, where albedo was computed for three large spectral bands only and from the properties of the first two layers (Brun et al., 1992; Vionnet et al., 2012).

TARTES is implemented as an optional module to be called instead of the original Crocus albedo scheme. This implementation has no significant impact on the model structure but increases the computation time of roughly a factor 10 depending on the number of snow layers and the snow depth.

TARTES makes use of four Crocus prognostic variables (specific surface area -- SSA, density, snow layer thickness and impurity content) and the angular and spectral characteristics of the incident radiance (e.g. the solar zenith angle and the presence of cloud cover). The computation of SSA has recently been implemented by \citet{carmagnola2014}.

The use of a full radiative transfer model embedded within the snowpack model enables the assimilation of the satellite reflectance data, therefore avoiding the introduction of

uncertainties from an external retrieval algorithm. And beyond its use for the assimilation of reflectances, TARTES also provides a more accurate calculation of light absorption parameters, leading to better simulations of the snowpack.

- In several places in the manuscript, the authors use the word "envelops" as a noun, but it is a verb. I think they mean "envelopes" instead in some (but not all) of these cases. Please rectify this word usage.

This has been modified in the new version of the manuscript. Thank you.

SPECIFIC COMMENTS

1. The second paragraph of the abstract (page 6830, lines 11-22) does not make it consistently clear that MODIS data are not actually used in the study. The first sentence suggests MODIS reflectance data are used, but the subsequent sentences refer to MODIS-like data. The authors need to include additional clarification here.

Both reviewers indicate the need to clarify that data are synthetic and/or this study is based on twin experiments. Some modifications were consequently done in the abstract, in the introduction and in section 4.2 "Nature of assimilated observations" (see below).

-----NEW-----: abstract

This paper examines the ability of optical reflectance data assimilation to improve snow depth and snow water equivalent simulations from a chain of models with the SAFRAN meteorological model driving the detailed multilayer snowpack model Crocus now including a two-stream radiative transfer model for snow, TARTES.

The direct use of reflectance data, allowed by TARTES, instead of higher level snow products, **mitigates** uncertainties due to commonly used retrieval algorithms.

Data assimilation is performed with an ensemble-based method, the Sequential Importance Resampling Particle filter, to represent simulation uncertainties. **In snowpack modeling, uncertainties of simulations are primarily assigned to meteorological forcings.** Here, a method of stochastic perturbation based on an autoregressive model is implemented to explicitly simulate the consequences of these uncertainties on the snowpack estimates.

Through twin experiments, the assimilation of synthetic spectral reflectances matching the MODerate resolution Imaging Spectroradiometer (MODIS) spectral bands is examined over five seasons at the Col du Lautaret, located in the French Alps. Overall, the assimilation of MODIS-like data reduces by 45\% the root mean square errors (RMSE) on snow depth and snow water equivalent. At this study site, the lack of MODIS data on cloudy days does not affect the assimilation performance significantly. The combined assimilation of MODIS-like reflectances and a few snow depth measurements throughout the 2010/2011 season further reduces RMSEs by roughly 70\%. This work suggests that the assimilation of optical reflectances has the potential to become an essential component of spatialized snowpack simulation and forecast systems. The assimilation of real MODIS data will be investigated in future works.

-----NEW-----: Intro

The work presented in this article examines the possibility, the relevance and the limitations of assimilating visible and near-infrared satellite reflectances into a multilayer snowpack model. A convenient approach, known as twin experiment, uses synthetic data in the same spectral bands than the real data, to examine the content of information of the observations, and the impacts we can expect from their assimilation. In twin experiments, the model used to create the synthetic data is the same as the model used for the assimilation. The synthetic observations are extracted from a member of the ensemble considered as the “true” state. Twin experiments are preferred in this first study in order to focus on the information content of the observations and to avoid the problem of observational biases.

Data assimilation is performed with a particle filter and a Sequential Importance Resampling (SIR) algorithm \citep{gordon1993,vanleeuwen2009,vanleeuwen2014}. The particle filter is easy to implement, free of hypotheses about the nature of the model and the observations, and provides uncertainties in the estimation of the snowpack state.

-----NEW-----: section 4.2

The first set of \textbf{synthetic observations} is composed of surface reflectances of the first seven bands of MODIS (central wavelengths : 460, 560, 640, 860, 1240, 1640, 2120 nm; \citealp{hall2007}). **In twin context, these synthetic observations are provided from the synthetic truth simulation running Crocus with its radiative TARTES model.**

Snow surface reflectances in the visible and near-infrared spectra are sensitive to the properties of the first millimeters to the first centimeters of the snowpack for a given wavelength \citep{li2001}.

2. The biases in shortwave and longwave radiation are of opposite sign (Table 1, left column). Does this reflect some specific shortcoming of SAFRAN, such as problems with a low bias in cloud conditions or a high bias in atmospheric transmissivity? In other words, are the radiation errors linked in some physical way, or is it just by chance that the biases are positive for shortwave and negative for longwave? Does vegetation/topographic shading at the CdP site factor into the positive SAFRAN shortwave bias, and does this influence the longwave estimation in any capacity? I recommend addressing these questions in the paragraph that discusses the discrepancies between SAFRAN and observations (page 6838, Lines 9-17). This paragraph currently focuses on temperature, precipitation, and wind speed but could be improved with more attention to the radiation components.

Some additional checks have revealed a higher bias (but of opposite sign) for longwave and shortwave radiation in case of clear sky, that may reflect a shortcoming in the atmospheric transmissivity calculation.

In addition, measured longwave fluxes are affected by vegetation and slopes while that is not considered in the SAFRAN longwave estimates. The altitude of clouds might also be too simplistically simulated in SAFRAN.

Concerning the shortwave radiation, a shading mask is applied to SAFRAN estimates to account for topographic and vegetation shading effects but the seasonal evolution of nearby vegetation is not taken into account in this correction.

Modifications were done in section 3.2 concerning this point (in bold below).

According also to review 2, specific comments 13 to 17, section 3.2 was rephrased as follows. (Answers to review 2, specific comments 13 to 17 are located directly bellow each comment.)

-----NEW----- **Section 3.2: Quantification of meteorological forcing uncertainties**

To quantify and calibrate the meteorological forcing uncertainties, we compare 18 years of surface meteorology from SAFRAN reanalysis with *in-situ* observations at the CdP. A long time-series from 1993 to present *morin2012* being available at this site, uncertainties in the SAFRAN meteorological reanalysis can be estimated.

Table [\ref{perturbed_forcing_stat}](#) (left column) reports the bias and the standard deviation of the difference between SAFRAN and the observations carried out at the CdP site, for each meteorological variable (the right column reports other data discussed later). The table reflects differences between SAFRAN and *in-situ* observations, resulting from the different spatial representativities of both sources, the intrinsic errors of the analysis system and measurement errors.

As highlighted by *quintana2008* who conducted an extended evaluation of SAFRAN reanalysis but over a shorter period (one year), the large discrepancies between the model and the observations can be explained by local effects due to orography and vegetation and, for the precipitation and wind speed, by the time interpolation necessary to obtain hourly forcing fields from the daily analysis. For example, the precipitation analysis is performed on a daily basis in order to include in the analysis the numerous rain gauges observations.

Radiation fluxes uncertainty might be attributed to biases in cloud coverage and altitude estimates, effects of vegetation and surrounding slopes that are not taken into account for longwave estimates. Finally, the shading mask for shortwave radiation does not account for vegetation evolution that can also lead to shortwave flux discrepancies. *durand2009* carried out, only on a limited set of variables, a more systematic evaluation of SAFRAN for the 1958-2002 period using 43 sites in the French Alps. Averaged over all locations, the RMSE on air temperature are similar to the one computed in our study. However, their results also highlight the spatial variability of SAFRAN performance (site RMSE ranges from -0.8 to +1.5 $^{\circ}\text{C}$). Nevertheless, this will not have a strong impact in this study since it is based on twin experiments.

3. I am unsure why the shortwave perturbations are additive while the longwave perturbations are multiplicative (page 6839, lines 8-10). Please clarify the logic behind this decision.

The reviewer is actually spotting a typo here: the perturbations was multiplicative for SW and additive for LW. The logic behind this is clarified in the new version of the manuscript, section 3.3, also reported after the answer to comment 4 below. Note that Section 3.3 has been entirely modified after comment 3, 4, and comments from Reviewer 2.

4. The authors rightfully attempt to maintain physical consistency amongst the meteorological variables (page 6839, Lines 16-19). Are any efforts made to examine the physical consistency

between shortwave and longwave radiation? For example, a high shortwave value and a high longwave value might not be physically realistic because the high shortwave implies no cloud cover whereas the high longwave value can imply cloud presence.

No, there is actually nothing done in the ensemble to preserve the physical consistency between the longwave and shortwave radiation. For real data assimilation, the physical consistency between the meteorological variables will be crucial: we plan to use forcing ensembles from meteorological ensemble simulations.

The limitations of our meteorological ensemble are further enlightened and discussed in the new section 3.3. "Building the ensemble of meteorological forcings".

New section 3.3 : “Building the ensemble of meteorological forcings”

The sample of meteorological forcings is formed by perturbing the original SAFRAN reanalysis with a random noise commensurate with the actual uncertainty. We thus build an ensemble of meteorological forcings with a negligible bias with respect to the SAFRAN reanalysis and a standard deviation close to the one computed from CdP statistics (Table \ref{perturbed_forcing_stat}, left column).

To keep the procedure simple and preserve physically consistent time variations of the forcings, the random perturbations are computed using a first-order autoregressive (AR(1)) model \citep{deodatis1988} for each variable:

$$X_t = \varphi X_{t-1} + \epsilon_t,$$

with X being the perturbation value at time t and $t-1$. φ is the AR(1) model parameter and can be written $\varphi = e^{-\frac{\Delta t}{\tau}}$, Δt being the time step and τ the decorrelation time.

Parameter τ is adjusted for each variable, so that the perturbed variable exhibits the same frequency of temporal variations than the original variable (Fig. \ref{Supp-Snowfall} bottom, in blue).

The amplitudes of the meteorological uncertainties are introduced with ϵ_t , a white noise process with zero mean and constant variance σ^2 . Variance σ^2 is computed from each standard deviation of the residuals between the reanalysis and observations at CdP (σ_{CdP} : Table \ref{perturbed_forcing_stat}, left column) following this equation:

$$\begin{equation} \sigma^2 = \sigma_{CdP} \times (1 - \varphi^2) \end{equation}$$

Finally, for each meteorological variable, the selection of an additive or multiplicative perturbation method is driven by (i) the nature of the variable (ii) the dependency of the model-measurement difference to the measured values as detailed below.

For precipitation rates, shortwave radiations and wind speed, the choice of a multiplicative method is motivated by the following reasons:

- SAFRAN reanalysis captures well the occurrence of precipitation (since it assimilates surface observation network) but are more subject to errors in the amount of precipitation;
- Regarding shortwave flux and wind speed, the model biases exhibit a linear dependency to the value of the variable (not shown). Consequently, a multiplicative method was selected.

For longwave radiation and air temperature, given that there is no dependency between the model biases and the field values, an addition method is chosen.

At every time step the perturbation X_t is applied as follows:

For the additive method, $variable_t = variable_t + X_t$; For the multiplicative method, the perturbation is centered on 1 (Y_t) before multiplying the variable.

$$Y_t = X_t + 1$$

$$variable_t = variable_t \times Y_t$$

For the multiplicative method, the perturbations are bounded by 0.5 and 1.5 to avoid extreme values. The result from this perturbation method is illustrated by Fig. \ref{Supp-Snowfall} which shows the snowfall rates over a one week period, as described by SAFRAN reanalysis, a realization of the perturbed analysis, and the full ensemble of perturbed analysis.

To maintain further physical consistency between the meteorological variables, snowfall is changed to rainfall if air temperature is higher than 274.5 K and the shortwave radiation is bounded to 200 W m^{-2} in case of rain or snow fall due to the inherent cloud cover. This behavior is consistent with the CdP statistics where over 18 years, during a precipitation period, the measured in situ shortwave radiation rarely exceeds $W \text{ m}^{-2}$.

Ensembles are generated with model errors coming from the statistics of the CdP site but as explained previously, the assimilation framework is based on the CdL area. Some adjustments in the building of ensembles are also required to take into account differences between these two areas.

In particular, the forest at CdP affects the local wind field and the radiative fluxes \citep{morin2012}, which explains a large part of the variability of SAFRAN errors at CdP. At CdL, an open meadow area, such variability is unlikely. To limit the overspreading of the forcing ensemble, the standard deviation used in the equation (3) for wind speed, short and longwave radiation are reduced to 0.6 m s^{-2} , 70 and 7 W m^{-2} , respectively, against 1.12 m s^{-2} , 79 and 24.5 W m^{-2} (Table \ref{perturbed_forcing_stat}, left column, values in brackets).

As shown in Table 1, the standard deviations computed from the generated ensemble (right column) are close to the ones prescribed to generate it (left column).

In the end, this stochastic method of perturbations makes possible the construction of an ensemble of perturbed forcings which are required when using ensemble methods.

The calibration of the perturbations are based on the CdP statistics while their temporal correlation is ensured by the AR(1) model.

The perturbation method exhibits some obvious limitations. Inter-variable correlations are indeed not taken into account in the ensemble except from the precipitation phase and the maximum value of short-wave radiation in case of precipitation. Adjustments to CdL are somewhat subjective, but this is not crucial in our twin experiment context since the considered truth will be simulated running Crocus with one forcing member drawn from this generated ensemble. A more physically consistent ensemble will be required when real data assimilation is investigated.

TECHNICAL CORRECTIONS

-1. Page 6830, Line 5: *Uncertainties can never be ruled out in any type of dataset; they can only be identified and reduced through improved datasets. Please rephrase.*

Correction done in Specific Comment 1

-2. Page 6830, Line 11 and Page 6832, Line 11: *The full name of MODIS is “MODerate resolution imaging spectroradiometer”. Please correct these lines.*

Thanks (both reviewers) to have seen this mistake.

Correction done in Specific Comment 1

- 3. Page 6831, Line 9: *Replace “reducing” with “reduce”.*

Done

-4. Page 6833, Line 6: *Should read “statistics”.*

Done

-5. Page 6833, Line 25: *Replace “including” with “includes”.*

Done

- 6. Page 6835, Line 21: *Replace “first” with “top” to be more specific to the location of these layers.*

Done

-7. Page 6837, Line 15: *The phrasing would sound better as “other physical parameterizations”.*

Done

- 8. Page 6839, Line 21: *Should read “captures”.*

Done

- 9. Page 6840, Line 4: *Based on Table 1, I think this should read “58.3” instead of “70”.*

No, 58.3 corresponds to the standard deviation obtained from the difference between the SAFRAN reanalysis with the generated ensemble for the shortwave flux. 70 is the value used in the normal distribution to generate it.

We added in brackets the adjusted standard deviation values (used to generate perturbations) in the table 1. The caption was modified as well. Details of these adjustments are given in the new section 3.3

Variables	CdP: Reanalysis - Observations		CdL: Reanalysis - Ensemble	
	Bias	std: σ_{CdP}	Bias	std: σ_{CdL}
Air temperature (C)	0.28	1.08	5.0 e-03	1.07
Wind speed (m s ⁻¹)	0.2	1.12 (0.6)	4.0 e-04	0.4
Shortwave radiation (W m ⁻²)	22.4	79 (70)	-3.1 e-03	58.3
Longwave radiation (W m ⁻²)	-14.0	24.5 (7)	2.0 e-02	7.0
Snowfall rate (kg m ⁻² h ⁻¹)	-2.0 e-02	0.4	5.0 e-03	0.1
Rainfall rate (kg m ⁻² h ⁻¹)	7.2 e-03	0.5	-5.0 e-03	0.1

Table 1. Bias and standard deviations (std) of the differences between SAFRAN reanalysis and *in-situ* observations (left) and the differences between SAFRAN reanalysis and the ensemble built up in the present study (right), for the perturbed meteorological forcings. The first set of statistics is derived from 18 years (1993-2011) of observations and reanalysis at the CdP and the second set is derived from our 300-members ensemble over the 2010/2011 hydrological season. **The values in brackets correspond to the adjusted standard deviation used to generate the ensemble at CdL site.**

-10. Page 6841, Line 17: What do you specifically mean here by the “spread” in the melt-out date? Is this the range (max-min) or the variance or some other statistic? A definition of uncertainty in melt-out date appears later (page 6844, Lines 13-14), so it might be helpful to bring this definition earlier in the text.

We meant the range. Since this was unclear, the following modification were done in the text, section 3.5 “Ensemble simulations”:

-----NEW-----

“The spread of the SD and SWE ensembles (Fig. 1b-c) is the largest at the end of the season, leading to a range of 24 days from the first to the last member to fully melt.”

Done

- 11. Page 6843, Line 16: Add “to” before “presenting”.

Done

- 12. Page 6846, Line 1: Should read “simpler” instead of “simplest”.

Done

-13. Page 6847, Line 8: Add “to” after “according”.

Done

- 14. Page 6849, Line 6: Should read “cloud coverage” instead of “clouds coverage”.

Done

- 15. Page 6850, Line 13: Rephrase to say “The ensemble spread retrieves almost the same value as. . .”

Following suggestions of both Reviewers (see review 2, Specific Comment 68), we modified the sentence this way:

-----NEW-----

The ensemble spread at the end of the season returns to almost the same value than the experiment without assimilation.

Done

- 16. Page 6854, Line 21: Add “as” before “MODIS”.

Done

- 17. Page 6854, Lines 22-23: Rephrase to say “Combining reflectance assimilation with SD assimilation at 4 dates during the snow season leads to. . .”

-----NEW-----

Combining reflectance assimilation with SD assimilation at 4 dates during the snow season leads to a decrease of SD and SWE RMSE by a factor close to 3.

Done

- 18. Page 6855, Line 11: Replace “what” with “which”.

Done

- 19. Page 6855, Line 18: Should read “through” instead of “though”.

Done

TABLE AND FIGURE COMMENTS

- Figure 1c: The upper limit of the vertical axis cuts off the SWE ensemble. Please extend so the entire ensemble can be seen.

Done

- Table 2: The understandability of this table would be improved if the column headings not only included the Figure reference, but also a brief description of what is represented in each experiment. For example, the “Fig. S2” column should also have a heading that says something like “Reflectance – all days” while the “Fig. S7” column should have a heading saying “SD – clear sky days”, etc. This will help the reader by not requiring them to keep searching for what is tested in each scenario.

Thank you for this welcome suggestion.

So we did some modifications, adding new lines (and a new column according review 2, specific comment 73) as displayed below:

Results reported in	Fig. 1	Fig. 3	Fig. S7	Fig. S2	Fig. S3	Fig. S4	Fig. S5	Fig. S6	Fig. S8	Fig. 5
Variable assimilated		Refl.	SD	Refl.	Refl.	Refl.	Refl.	Refl.	Refl. + SD	Refl.
Assimilation timing	No AD	Baseline	Clear sky days	All days	Accu.	Melt	Before Snowf	After Snowf		All seasons
SD (m)	0.13	0.07	0.03	0.05	0.05	0.12	0.07	0.12	0.04	0.07
SWE (kg m ⁻²)	35.4	19.7	7.4	14.4	12.9	35.5	21.8	37.2	9.6	20.2

Table 2. SD and SWE seasonal averaged RMSE computed with respect to the synthetic truth for all experiments over the 2010/2011 season. Results reported in Fig. 5 are the RMSE computed over the 5 selected seasons.

ANONYMOUS, REVIEW 2

General Comments:

The study is important and relevant in that it has showed the potential usefulness of assimilating reflectance data into a snow model. The design of experiments appears to be well thought out, and the results of the sensitivity experiments are particularly interesting. The presentation of procedures carried out is sometimes unclear. The study is scientifically sound, and most of the comments relate to making the presentation more clear. I feel the paper should be published after relatively minor changes discussed below:

1. The abstract be specific as to the procedures that were carried out. It should make clear from the outset that the authors are examining the usefulness of assimilating reflectance data, but are not using real reflectance data during assimilation. The Crocus model should be mentioned as the model used to calculate snow depth, and the source of meteorological inputs (SAFRAN), as well as the method used to generate an ensemble of input forcing should be mentioned.

The abstract has been modified accordingly.

See details provided in reviewer 1, Specific Comment 1

2. It should be clear throughout the paper wherever “observations” are synthetic observations derived from model results. In these instances “truth” should be changed to “synthetic truth” and “observations” to “synthetic observations”, etc.

The 2 reviewers attest the need to clarify that this study is based on twin experiments with synthetic data. To this end, we also added a paragraph in the introduction section to present what the twin experiment method is. Also we changed “truth” to “synthetic truth” and “observations” to “synthetic observations”.

See details provided in reviewer 1, Specific Comment 1

3. A paper describing the potential for assimilating MODIS data in a distributed way over the Greenland Ice Sheet has been recently published (Navari et al., 2015), but discusses assimilation of ice surface temperature data derived from MODIS (i.e. in a different part of the electromagnetic spectrum). Since that study also uses MODIS data (albeit in a different way with far infrared measurements from MODIS) it could be referred to in the introduction. Navari, M. Margulis, S. A., Bateni, S. M., Tedesco, M., Alexander, P., and Fettweis, X.: Feasibility of improving a priori regional climate model estimates of Greenland ice sheet surface mass loss through assimilation of measured ice surface temperatures, *The Cryosphere*, 10, 103-120, doi: 10.5194/tc-10-103-2016, 2016.

Thank you for the reference.

The reference has been added in the introduction:

See review1, General Comment 1.

4. The application of errors from Col de Porte at Col de Lautaret needs more discussion. The methods used to adjust errors from one site to the other site should be discussed in more detail, perhaps in the supplement.

A more detailed discussion on this adjustment has been added in the new section 3.3. (see modifications in response of Review 1, Specific Comments 3 & 4.

5. The comparison between the ensemble of simulations at CdL and RMSE at multiple locations seems unfair in that the spatial distribution of snow depth errors is not necessarily the same as the distribution of errors associated with errors in input forcing. As the authors mentioned, errors at CdP and CdL are different partly because of differences between the sites (forested vs. open). It seems likely that errors in SND at CdL will be smaller than those at other locations because of the lack of forest cover. Therefore I don't see the purpose of the comparison described in Section 3.5, except perhaps to illustrate that errors may be larger when considering multiple locations, and therefore, perturbations may need to be adjusted spatially in future use of "real" data assimilation. It may make more sense to create an ensemble at CdP, and to see whether the ensemble method captures the RSME of SND at that particular location, given the known uncertainties in forcing data at CdP. This would somewhat validate the method being used to generate errors in SND and other variables. Following your suggestion, we created an ensemble at CdP and reported the results on new Figure 2.

The section 3.6 "Dispersion of the ensemble of Crocus simulations" has become as follows.

-----NEW-----

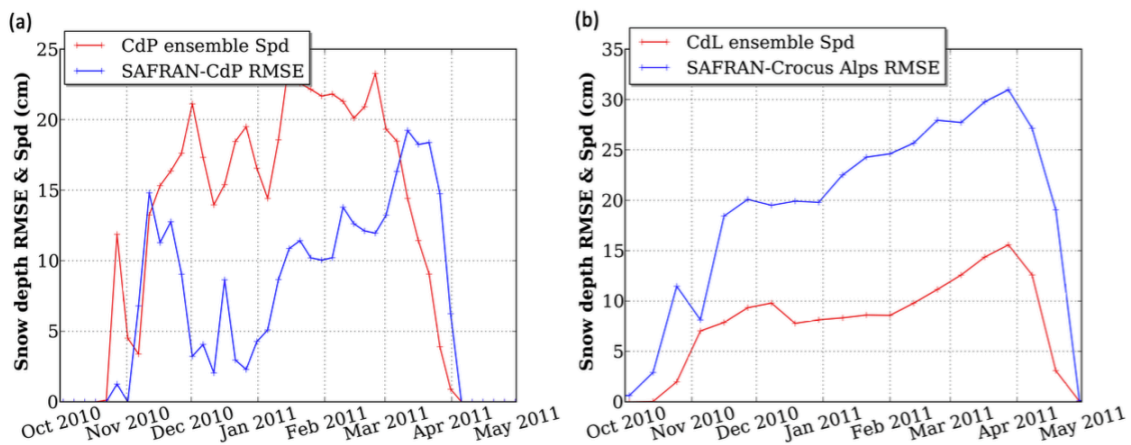


Figure 2. Time evolution over the 2010/2011 season of (in red) the SD ensemble Spd with respect to the ensemble mean and (in blue) the SD RMSE between SAFRAN-Crocus estimates and *in-situ* observations. (a) for the CdP site and (b) for the CdL ensemble compared to the multiple Alps stations at the same elevation than CdL.

Here we assess whether our ensemble represents a realistic spread of SD over time with respect to previous evaluations of the model through a spread-skill plot.

Given that no SD measurements were systematically carried out at the CdL site, we were not able to evaluate our ensemble spread from SAFRAN-Crocus simulations with a time series of *in-situ* measurements at this site. But, as demonstrated by [fortin2014](#), the ability

of the ensemble spread to depict the simulation error can be evaluated by the comparison of the root-mean-squared error (RMSE) and the ensemble spread (Spd) with respect to the ensemble mean.

Firstly, using the method previously described, an ensemble of Crocus simulations was carried out at the CdP site with no adjustment on CdP statistics to evaluate the relevance of our perturbation method by comparing the RMSE between SAFRAN-Crocus simulation and in situ measurements with the Spd of the CdP ensemble. Then, we compare the Spd of our ensemble simulation at the CdL site with a SAFRAN-Crocus RMSE computed from the difference between SD Crocus estimates with in situ SD measurements across multiple stations (at the same elevation than CdL). We used roughly 60 daily snow depth measurements stations from the M\et\eo-France observation stations network (only stations within the same altitude range as the CdL site (1800 - 2200m a.s.l.)).

The multiple station RMSE and Spd terms are defined as follows, for a variable X ,

$$\text{RMSE}(X) = \left(\frac{1}{M} \sum_{t=1}^M \frac{1}{N_k} \sum_{k=1}^{N_k} (X_{t,k}^{\text{model}} - X_{t,k}^{\text{in situ}})^2 \right)^{1/2},$$

$$\text{Spd}(X) = \left(\frac{1}{M} \sum_{t=1}^M \frac{1}{N_e} \sum_{n=1}^{N_e} (X_{t,n} - \bar{X}_t)^2 \right)^{1/2},$$

where M represents the number of time steps, N_e the size of the ensemble and N_k the number of in situ measurements. The SD value of the ensemble member n at the date k is $X_{t,n}$ and \bar{X}_t is the mean of the ensemble at the date t .

The value from SAFRAN-Crocus simulation at the site measurement k and at the date t is given by $X_{t,k}^{\text{model}}$, and $X_{t,k}^{\text{in situ}}$ is the value from the in situ SD measurement. RMSE and Spd are computed at observation times.

For comparisons based on only one point, the RMSE equation for a variable X becomes:

$$\text{RMSE}(X) = \left(\frac{1}{M} \sum_{t=1}^M (X_t^{\text{model}} - X_t^{\text{in situ}})^2 \right)^{1/2},$$

Figure \ref{dispersion} (a) shows that at the CdP site the SD dispersion (Spd) of the ensemble is consistent with the RMSE between SAFRAN-Crocus simulation with respect to in situ measurements at this site. This suggests that our perturbation method is able to represent the forcing uncertainties on snowpack simulations. Nevertheless, concerning the CdL area over the 2010/2011 season, the SAFRAN-Crocus RMSE is roughly two times higher than the SD

dispersion (Spd) of our ensemble (**Fig. \ref{dispersion} (b)**). This means that our ensemble is under-dispersive in terms of SD. This may be partly explained by the calibration of perturbations, based on statistics at a location (CdP) which is not highly affected by wind erosion/accumulation in contrast to many other measurement sites. In addition, only meteorological errors are considered in our ensemble whereas the other model errors also contribute to the simulation error.

Nonetheless, given that experiments in the present work are twin and that the observations are selected within the ensemble (synthetic observations), the impact of this under dispersion is not crucial, but will be considered when using real data.

Specific Comments:

1. P. 6830, Lines 7-8: This sentence is unclear. I'm not sure what is meant by "essentially ascribed". Inclusion of details discussed in the general comments section may allow this sentence to be modified or replaced.

Some modifications were carried out in the abstract, see review 1: Specific Comment 1.

Also, more details are given at the beginning of the section 3.1:

"As shown in Raleigh et al. (2015), the meteorological forcings are the major source of uncertainty in snowpack simulations when a meteorological model is used to drive the snow model."

2. P. 6830, Line 11: Perhaps this sentence can be modified to make it more clear that the reflectances are not real: "The assimilation of synthetic spectral reflectances, designed to match the spectral resolution of the MODerate resolution Imaging Spectroradiometer..." Also note the correct name for MODIS.

Done

See review 1: Specific Comment 1 & Technical Correction 2

3. P. 6830, Lines 19-21: Since real data have not been assimilated yet, perhaps this statement is slightly too strong. "Should become" could be changed to "has the potential to become" or something similar.

Done

4. P. 6833, Lines 8-10: Perhaps here, the forcing data used at Col de Lautaret can be introduced, and the method of generating an ensemble of forcing can be briefly noted as well.

Done

-----NEW-----

For this reason, assimilation experiments are carried out at the Col du Lautaret (CdL) located (2058 m a.s.l.) in the Ecrins area, France, which exhibits a large flat open area, above treeline, more suitable for remote sensing. **Consequently, an ensemble of perturbed forcing was generated in order to represent the range of possible weather conditions at the CdL area. To this end, we developed a stochastic method using a first-order autoregressive model based on the estimated meteorological uncertainty.**

5. P. 6833, Line 18: Change "reflectance observations" to "synthetic reflectance observations". Perhaps also change "one point" to "CdL".

Done

6. P. 6833, Line 19: Suggest changing "this previous experiment" to "the reference experiment"

Done

7. P. 6834, Lines 26-27: Over what period is this threshold applied, a single model time step? *The procedure of layering is activated at the beginning of each time step (15 minutes in our case)*

-----NEW-----

For a snowfall on an existing snowpack, fresh snow is incorporated into the top layer if (i) snow microstructure characteristics are similar, (ii) the top layer is thinner than 1cm and (iii) the snowfall intensity is inferior to 0.03 kg.m⁻².h⁻¹. If one of these criteria is not met or change during the time step, a new top layer is created.

Done

Does the threshold change if the time step also changes?

Actually it does not, but we do not usually change the time step either.

8. P. 6835, Line 1: Change “identical layers” to “a set of identical layers” for clarity.

Done

9. P. 6835, Lines 5-7: Change “layer that is too small relatively” to “layers that are too small relative”, and change “is aggregated with an adjacent one” to “are aggregated with adjacent ones”. *Done*

Is the “optimal vertical profile” an optimal profile of layer thicknesses?

How is this optimal profile determined?

We directly included the answer into the paragraph.

-----NEW-----

In absence of snowfall, the model seeks first to merge two thin and adjacent layers with similar microstructure characteristics, or inversely, split the thick ones.

When the number of layers has reached a maximum of 50, layers that are too small relative to a prescribed optimal vertical profile are aggregated with adjacent ones. **This idealized thickness profile depends on the current snow depth and on the user-defined maximal number of layers. To reach the optimal vertical profile, the model first seeks to thin the top layers, most subject to the exchange of energy, and then to keep an appropriate thickness ratio between adjacent snow layers to prevent numerical instabilities in the resolution of the heat diffusion equation through the snowpack**

10. P. 6836, Line 24: Please spell out the acronym SAFRAN.

Système d’Analyse Fournissant des Renseignements Atmosphériques à la Neige

This has been added in the new version of the manuscript.

Also a few more details about SAFRAN would be appreciated, for instance, what kinds of observations go into the product, and what is its spatial resolution?

Done, see modification below

-----NEW-----

The snowpack evolution strongly depends on near-surface meteorological forcings. These forcings are provided by the meteorological downscaling and analysis tool SAFRAN (**Système d’Analyse Fournissant des Renseignements Atmosphériques à la Neige** \citep{durand1993}). SAFRAN is used to drive snowpack simulations in the French mountains because it is designed to operate at the geographical scale of meteorologically homogeneous mountain ranges, varying from 400 to 2000km². The model combines vertical profile estimates from the ERA-40 re-analysis with observed weather data from the automatic surface observations network at different elevations, the French Snow/Weather network, rain radars, and rain gauges. As

outputs, SAFRAN provides meteorological data to the snowpack model with an hourly time step for all slopes and aspects, and a 300 m-elevation step.

11. P. 6837, Line 9: The phrase “simulate the errors” is a bit confusing... perhaps you mean that you need to first simulate the impact of errors on the simulation of the snowpack?

Yes that is what it means. This has been clarified in the new version of the manuscript as reported below.

-----NEW-----

In view of assimilating observations to reduce snowpack simulation uncertainties, we first need to **represent them**.

12. P. 6837, Lines 14-16: Perhaps provide further explanation as to why these errors are not considered. I would imagine these errors are difficult to evaluate as they may vary by location and may be difficult to separate from other sources of error. Can the authors briefly comment on how their inclusion might affect the results presented?

We follow Raleigh et al. (2015) by considering the forcings as the only source of uncertainty. Obviously, this is an approximation. We did not consider model errors because they are indeed more difficult to characterize and represent, notwithstanding their spatial variations that would be ignored here. The manpower needed to implement their effects has been spared for this first study focused on the relevance of reflectance assimilation. But of course, this question will have to be addressed with real data. This is (more briefly) stated in the new version of the manuscript, section 3.1.

-----NEW-----

Snowpack model errors introduced by metamorphism and other parameterizations of physical laws are not taken into account here. The characterization and representation of these errors, notably in the perspective of real data assimilation, will be addressed in a future and dedicated work. An identified option is to use multi-physics ensemble simulations.

13. P. 6838, Line 3: I think it would be better to refer to RMSE rather than the “standard deviation of the difference”, for consistency with other portions of the paper.

The standard deviation of the difference is computed by subtracting the mean, contrary to the RMSE. Since these are different quantities, we suggest to keep the text as is.

14. P. 6838, Line 5: Does “significant” refer to statistical significance? Please clarify.

No, actually we did not make statistical tests. Significant has been consequently removed from the sentence.

“The table **reflects differences** between..”

Done, See Review 1, Specific Comment 2.

15. P. 6838, Lines 6-8: Differences can also occur because of measurement errors at CdP.

True, this has been added in the new manuscript.

Done, See Review 1, Specific Comment 2.

16. P. 6838, Line 13: Hourly interpolation of the daily analysis wasn't discussed earlier. Please elaborate.

Done, See Review 1, Specific Comment 2.

17. P. 6838, Lines 15-17: This sentence is unclear. What is the average RMSE or range of RMSE values at the stations?

Which study highlights the spatial variability of SAFRAN? I presume it is the Durand et al. (2009) study, but this is not clear from the sentence. How much do the RMSEs change across stations?

All these information are provided in Durand et al., 2009. Averaged on 43 sites, the values of RMS temperature observation error range from 1° to 1.5°C over the 1959 – 2001 period.

But at the same time, over the whole period, the statistics between SAFRAN and in situ air temperature can be quite different from a site to another. For example, at the Lus La Croix Haute site the bias and rms are respectively, +0.2 and 1.2°C while at the barcelonnette site we note +1.1 and 5.8°C.

What are the implications of this spatial variability for this study; i.e. can the uncertainty estimates at CdP really be used as indicators of the uncertainty at CdL?

Regarding the above arguments, it should have been more convenient to quantify uncertainty directly at the CdL area but this site does not provide a time-series of meteorological forcing.

Consequently, since the CdP site is the most instrumented area overs 20 years in the French Alps, the use of the CdP statistics was the best option to get an estimate of the meteorological uncertainty. Given that CdP and CdL are not located in the same mountain range (respectively, Chartreuse mountain range and Grandes Rousses mountain range) and at the same altitude, some adjustments were carried out on the perturbations, as explained in section 3.3.

The possible error introduced from this variation will not have a strong impact in this study since it is based on twin experiments. A more physically consistent ensemble should be built for future work with real data.

This has been added in the new version of the manuscript.

The Section 3.2 was rephrased and presented in Review 1, Specific Comment 2. The modifications concerning this comment are reported below:

-----NEW-----

\cite{durand2009} carried out, only on a limited set of variables, a more systematic evaluation of SAFRAN for the 1958-2002 period using 43 sites in the French Alps. Averaged over all locations, the RMSE on air temperature are similar to the one computed in our study. However, their results also highlight the spatial variability of SAFRAN performance (site RMSE ranges from -0.8 to +1.5 \textdegree C). Nevertheless, this will not have a strong impact in this study since it is based on twin experiments.

Comments 18 to 28: See Review 1, Specific Comments 3 & 4.

The whole section 3.3 was modified taking into account these comments.

18. P. 6839, Line 2: Mention how tau is chosen here rather than later on.

Comments 18 to 28: See Review 1, Specific Comments 3 & 4.

The whole section 3.3 was modified taking into account these comments.

19. P. 6839, Line 6: Some formulas should be included describing how a given variable at a given time step is perturbed (through either multiplication or addition).

Comments 18 to 28: See Review 1, Specific Comments 3 & 4.

The whole section 3.3 was modified taking into account these comments.

20. P. 6839, Lines 7-8: What is meant by “the nature of the variable”? It becomes a bit clearer later on, e.g. precipitation should not be additively perturbed to avoid creating precipitation where there is none. Can the authors be more specific? The second criteria is also unclear and does not seem to be mentioned later. Please provide a more detailed description of how a method is chosen for a given variable.

Comments 18 to 28: See Review 1, Specific Comments 3 & 4.

The whole section 3.3 was modified taking into account these comments.

21. P. 6839, Lines 14-16: I suggest discussing how tau is adjusted when tau is introduced in the previous paragraph. More details should be provided as to how tau is chosen, i.e. how is it determined that the “temporal variation” of perturbed variables is similar to that of the original variables?

Comments 18 to 28: See Review 1, Specific Comments 3 & 4.

The whole section 3.3 was modified taking into account these comments.

22. P. 6839, Lines 18-19: Suggest saying that the maximum value of shortwave radiation is set to 200 W m⁻² for clarity. Is this Done because of the presence of clouds? Please make this clear.

Comments 18 to 28: See Review 1, Specific Comments 3 & 4.

The whole section 3.3 was modified taking into account these comments.

23. P. 6839, Lines 20-23: This is out of place here, and should be mentioned earlier in the previous paragraph.

Comments 18 to 28: See Review 1, Specific Comments 3 & 4.

The whole section 3.3 was modified taking into account these comments.

24. P. 6839, Lines 27-29: Suggest modifying this sentence for clarity: “In particular a forested area masks a portion of the shortwave radiation at the CdP site, and modifies the local wind field. The model does not account for this forested area, resulting in the large discrepancies between model and observations.”

Comments 18 to 28: See Review 1, Specific Comments 3 & 4.

The whole section 3.3 was modified taking into account these comments.

25. P. 6840, Lines 1-4: The procedure for these adjustments should be provided, along with the results of the sensitivity tests if possible, in the supplementary material.

Also, the standard deviation for wind speed appears to be different. Was this also adjusted?

Thank you to have seen this mistake.

This was added in the new section 3.3.

Comments 18 to 28: See Review 1, Specific Comments 3 & 4.

26. P. 6840, Lines 5-6: Actually the standard deviations used to generate the ensemble are not provided in the left column, as they have been adjusted for the new location. I suggest adding another column showing the prescribed standard deviations for CdL. Also perhaps this is best mentioned after mentioning the use of an ensemble in the next paragraph.

Instead adding a new column, we just add the adjusted standard deviation used to generate the ensemble in brackets for the variables for each the standard deviation was adjusted. This is now detailed in the new version of Table 1 legend.

Variables	CdP: Reanalysis - Observations		CdL: Reanalysis - Ensemble	
	Bias	std: σ_{CdP}	Bias	std: σ_{CdL}
Air temperature (C)	0.28	1.08	5.0 e-03	1.07
Wind speed (m s ⁻¹)	0.2	1.12 (0.6)	4.0 e-04	0.4
Shortwave radiation (W m ⁻²)	22.4	79 (70)	-3.1 e-03	58.3
Longwave radiation (W m ⁻²)	-14.0	24.5 (7)	2.0 e-02	7.0
Snowfall rate (kg m ⁻² h ⁻¹)	-2.0 e-02	0.4	5.0 e-03	0.1
Rainfall rate (kg m ⁻² h ⁻¹)	7.2 e-03	0.5	-5.0 e-03	0.1

Table 1. Bias and standard deviations (std) of the differences between SAFRAN reanalysis and *in-situ* observations (left) and the differences between SAFRAN reanalysis and the ensemble built up in the present study (right), for the perturbed meteorological forcings. The first set of statistics is derived from 18 years (1993-2011) of observations and reanalysis at the CdP and the second set is derived from our 300-members ensemble over the 2010/2011 hydrological season. **The values in brackets correspond to the adjusted standard deviation used to generate the ensemble at CdL site.**

27. P. 6840, Lines 12-13: It would be helpful to remind the reader here how these are taken into account in this case.

Comments 18 to 28: See Review 1, Specific Comments 3 & 4.

The whole section 3.3 was modified taking into account these comments.

28. P. 6840, Lines 13-14: Explain why it is not crucial to account for intervariable correlations for the purposes of this experiment.

Comments 18 to 28: See Review 1, Specific Comments 3 & 4.

The whole section 3.3 was modified taking into account these comments.

29. P. 6841, Lines 1-3: Are the impurity concentrations consistent with any previous measurements of snow impurity content?

The dry deposition flux varies from 0 to 0.5 ng g⁻¹ s⁻¹ with a median value is 0.015 ng g⁻¹ s⁻¹ in concentration which roughly corresponds to 3.5 kg m² s⁻¹. This is the same order of magnitude than the dry deposition rates obtained for this location using ALADIN-Climat (Nabat et al., 2015) simulations. We however prefer not to include this discussion in the paper since the comparison required more detailed analysis and field measurements and since it not the main objective of our study.

30. P. 6841, Lines 8-13: The details of the figure could be shortened somewhat since they are already mentioned in the figure caption.

Done

-----NEW-----

Figure \ref{run_init} presents **the result of the ensemble simulation with 300 members (represented by the black lines).**

The simulation forced by the unperturbed reanalysis (**red line**) is included within the envelope of the ensemble. The spread of the ensemble reflects the consequences of possible overestimations and underestimations of meteorological data by the reanalysis.

31. P. 6841, Lines 17-18: Change “dispersion range (Δ SWE \approx 300 kg m⁻²)” to “dispersion range of SWE (Δ SWE \approx 300 kg m⁻²)”

Done

32. P. 6841, Lines 18-19: It would be better to refer to the snowpack here: “The snowpack in some ensemble members has just started to melt, while in other cases, the snowpack has already disappeared.”

Done

33. P. 6842, Line 11: It seems that the RMSE is calculated as a RMSE for modeled vs. in situ snow depths across multiple stations. Please clarify what the RMSE refers to here.

See Review 2, General Comment 5.

34. P. 6842, Line 14: The letter n was used in the equation for Spd as an indicator of the ensemble number. Here, I believe it refers to neither time, nor ensemble member, but to a station identifier, and M is the total number of stations, at a given time. Please clarify and change the notation to avoid confusion.

See Review 2, General Comment 5.

35. P. 6842, Line 18: It is not clear what the “reference” is at this point. Perhaps replace with “a synthetic true reference simulation”

See Review 2, General Comment 5.

36. P. 6842, Lines 19-21: Since observations are not mentioned yet, perhaps this should be moved to the next paragraph.

See Review 2, General Comment 5.

37. P. 6843, Line 11: The term “twin” has not been defined yet. It would be helpful to define it here rather than later on for those readers not familiar with the terminology.

A description of twin experiment was added in the introduction section.

See Review 1, Specific Comment 1

38. P. 6843, Line 19: Perhaps change “more physics details” to “further details”.

Done

39. P. 6843, Line 22: Again I think it would be better to mention this in section 3.6.

The aim of section 3.6 is only to evaluate the dispersion of the ensemble from the stochastic perturbation method. We prefer keeping this sentence with its idea at the beginning of the section 4.1 General settings and diagnostics.

40. P. 6843, Line 23: But the synthetic observations come from the same model into which data are being assimilated. The model is not independent. Please revise, and clarify that the synthetic observations come from a single Crocus ensemble member.

Done, see modification below

-----**NEW**-----

The assimilation experiments are twin, meaning that the observations are synthetic and come **from a single model simulation**. They are performed over five winter seasons at the CdL area.

41. P. 6844, Line 1: I suggest changing “control simulation” to “synthetic truth simulation” for clarity, here and in other places where it is mentioned.

Done

42. P. 6844, Line 2: Perhaps change “virtual observations” to “synthetic observations” for clarity.

Done

43. P. 6844, Lines 2-4: It may be helpful to mention the virtual or synthetic observations extracted from the simulations. In particular it would be helpful to mention (for understanding the following section) that synthetic reflectance observations are obtained from Crocus, through the use of the TARTES model.

-----**NEW**-----

A synthetic truth simulation is first obtained running Crocus, **through the use of the radiative transfer model TARTES**, forced by one perturbed meteorological forcing, as detailed in Section \ref{sec_pert}.

Done

44. P. 6844, Line 7: Change “truth” to “synthetic truth” for clarity.

Done

45. P. 6844, Lines 6-8: Suggested change to the sentence: “Data assimilation performances are evaluated by comparing RMSE for ensembles with and without assimilation, and by comparing the synthetic true simulation to the 33rd, 50th, and 67th quantiles from the ensembles with assimilation.”

Done

46. P. 6844, Lines 16-18: Mention that these are derived using TARTES in Crocus.

-----**NEW**-----

The first set of **synthetic** observations is composed of surface reflectances of the first seven bands of MODIS (central wavelengths: 460, 560, 640, 860, 1240, 1640, 2120 nm;

\citealp{hall2007}). In twin context, these synthetic observations are provided from the synthetic truth simulation running Crocus with its radiative TARTES model.

47. P. 6845, Lines 5-6: I suggest moving this sentence to the end of the paragraph.

-----NEW-----

The setup designed in our study (one point, twin experiments) allows relevant comparisons of the benefits of assimilating separately or jointly the two above mentioned types of observations. **For future works assimilating real data, the difference in the geometrical configuration between the simulated TARTES reflectances and satellite observations will be addressed.**

48. P. 6846, Lines 24-25: The sentence is unclear. Suggested change: "Inversely, a new perturbed forcing is assigned to a duplicated particle for propagation to the next analysis."

Done

49. P. 6847, Line 7: How are these "clear sky days" chosen? Are these based on the real measurements at CdL, or are they from real MODIS data? Please clarify.

Actually we use real MODIS data to do it. As other possible variables (albedo, NDSI, reflectance..) a cloud mask can be estimated from MODIS radiance data using the algorithm named MODimLAB (Sirguey et al., 2009).

-----NEW-----

To mimic real cloud conditions, reflectances are assimilated at 34 clear sky days of the season. **We define a clear sky date according to the real cloud mask from MODIS data computed with the method of Sirguey et al. (2009).**

50. P. 6847, Lines 8-9: Are real MODIS data used in this case? If so, please provide details about MODIS data in an earlier section. If not, I think this sentence can be removed, because this study does not make use of real MODIS data.

See response to the previous comment.

51. P. 6847, Line 13: Clarify that the envelopes are the envelopes from SD and SWE ensembles for the baseline experiment (e.g. "SD and SWE ensembles for the baseline experiment...")

Done

52. P. 6847, Lines 17-18: Suggest changing sentence to: "This is observed in Fig. 3, where the baseline experiment envelopes (blue shading) are narrower than those of the ensemble without assimilation (grey shading)."

Done

53. P. 6847, Lines 21-23: Mention the terms "forecast" and "analysis" to be consistent with Figure 4.

Fig 4, RMSE curves: "(Blue solid line: forecast; blue dotted line: analysis)".

-----NEW-----

Figure \ref{RMSE_8009} shows the time evolution of the RMSE with assimilation at every observation time, **at the end of the forecast step (blue solid line)** and just after the filter analysis (**blue dotted line**). These results are compared to the RMSE without assimilation (grey lines).

54. P. 6848, Line 1: What is meant by “the continuous flow of observations”? I think the authors mean to indicate that the observations are well distributed in time. Please clarify.

Yes, see modification below

-----NEW-----

The reduced RMSEs with assimilation are consequently due **to the successive observations throughout the season**, highlighting the role of model dynamics.

55. P. 6848, Lines 4-5: Change “extended and unobserved periods without precipitation” to “extended periods without precipitation and without available observations”

Done

56. P. 6848, Line 11: Which figure should we refer to for the example on 28 January?

Done

-----NEW-----

(**Fig. 3**, for example, on 28/01/2011)

57. P. 6848, Line 19: Change “the whole ensemble to a unique set” to “all ensemble members to the same set”

Done

58. P. 6848, Line 20: Change “discrimination between members impossible only from the reflectances” to “discrimination between members using reflectances alone impossible”

Done

59. P. 6848, Line 21: Change “the analysis” to “the subsequent analysis”

Done

60. P. 6848, Line 22: Again, which figure should be examined here?

Fig 3, Done

61. P. 6848, Line 28: Change “at the end” to “towards the end”.

Done

62. P. 6848, Lines 2-4: This statement is not really supported by the previous analysis, although it is shown that this is important later. Either note that this will be shown later, or remove this sentence.

Done

Ok, this has been reformulated as follows:

-----NEW-----

The strongest RMSE reductions occur right after extended periods without precipitation and without available observations, when the reflectance ensemble spread is particularly

pronounced (e.g. Fig 3a). During these periods (e.g. from 07/12/2010 to 14/12/2010, or from 11/01/2011 to 21/01/2011), the ensemble uncertainties on reflectances, SD and SWE grow under the influence of the perturbed forcings including the perturbed impurity deposition rate.

63. P. 6849, Line 8: Suggest changing “impact of the limited number of available data” to “impact of limiting the number of available observations” for clarity.

Done

64. P. 6849, Lines 9-10: Change “first one” to “baseline experiment” for clarity. *Done*
Change “...carried out but assimilating an observation” to “...carried out, but assimilation is performed...”.

Done

65. P. 6849, Line 15: As the envelope for the experiment is wider than the reference experiment, I think it is an overstatement to say that the fit is “perfect”.

Done

-----NEW-----

Obviously, in this second experiment, **concerning the 640-nm reflectance variable, the spread of the ensemble is greatly reduced, well fitting the observations (red dots) and its envelope does not show any extended periods with a large range of reflectance values anymore (Fig. \ref{Supp-FP_8017} a).**

66. P. 6849, Line 23: Change “that the limited number” to “that assimilating a limited number” for clarity.

Done

67. P. 6850, Line 7-10: Is it possible to give each of these simulations a meaningful name? This would be very helpful when references are made to each simulation in the paper. Otherwise the reader forgets the details of the simulation. If the authors think it would be more confusing to name each simulation, the details should be briefly mentioned when describing the results, e.g. “In case (i), where assimilation occurs only at the beginning of the season, results show...”

Done, see modification below

(Table 2, was modified accordingly. See Review1 Table and Figure Comments)

-----NEW-----

The baseline experiment suggests that the timing of observations may largely determine the quality of the assimilation process. To explore the role of the timing, four additional assimilation tests are designed for which MODIS-like reflectances are assimilated (i) only at the beginning of the season (before 31/12/2010, Fig. \ref{Supp-FP_8018}: **Accu**), (ii) only in the second part of the snow season (after 31/12/2010, Fig. \ref{Supp-FP_8019}: **Melt**), (iii) only after several day-long periods without precipitations (Fig. \ref{Supp-FP_8020}: **Before Snowf**) and (iv) only right after snowfalls (Fig. \ref{Supp-FP_8026}: **After Snowf**).

In case (i: **Accu**), results show that even if the SD and SWE spreads are reduced during the assimilation period, the assimilation has almost no effect on the snow estimates during the snow melt. The ensemble spread retrieves to almost the same value than the experiment without assimilation. The uncertainty of the snow melt-out date is reduced to 22 days only, in comparison with 24 days without assimilation. As for case (ii: **Melt**), the spread reduction becomes quite discernible roughly 2 months after the first assimilation date and never reaches the value of the baseline experiment. The uncertainty of the snow melt-out date is however reduced to 11 days. This demonstrates that it is essential to assimilate reflectances over the entire season to compensate the fast growth of the snowpack ensemble in response to the uncertainties in the meteorological forcing.

In both cases (iii: **Before Snowf**) and (iv: **After Snowf**), reflectances are assimilated at only 7 dates of the season. Case (iii: **Before Snowf**) exhibits a more pronounced SD and SWE spreads reduction compared to case (iv: **After Snowf**). The uncertainty on the snow melt-out date drops to 9 days in case (iii: **Before Snowf**) while it stays at 23 days in case (iv: **After Snowf**). In absence of precipitation, the snow surface is aging, leading to a decrease of reflectance values and a spread of the reflectance ensemble (Fig. \ref{Supp-FP_8020} a).

68. P. 6850, Line 13: Change “ensemble spread retrieves” to “ensemble spread at the end of the season returns”

Done

-----NEW-----

The ensemble spread at the end of the season returns almost the same value as the experiment without assimilation.

69. P. 6851, Lines 20-21: This sentence seems a bit out of place. Perhaps it can be moved to the end of the paragraph and expanded on a bit.

We followed your suggestion and added a new paragraph at the end of the section.

-----NEW-----

Figure \ref{RMSE_5seasons} also shows that, all these findings obtained for the 2010/2011 season are also verified for the five studied seasons. All assimilation experiments of synthetic SD observations reduce the RMSE with respect to both the model run without assimilation (red lines) and the experiments assimilation synthetic reflectances data (blue lines). However, in case of shallow snowpack, the better performance is obtained using reflectance data.

70. P. 6852, Line 5: The snowpack is probably also more sensitive to absorbed solar radiation. We are unsure what the reviewer is meaning here. In case of thin snowpack more solar radiation may be absorbed by the soil. No change

71. P. 6852, Lines 13-14: Although this seems likely, I’m not sure what evidence from the experiments that were Done supports this statement.

This statement is supported by the fact that every SD observations assimilation reduces the envelops independently of the precipitation events and which is not the case for reflectance (Fig S7). This is now detailed in the modified version below.

-----NEW-----

Excepted for thin snow cover, the assimilation of SD observations outperforms reflectance assimilation in terms of SWE and SD estimates and seems to be less affected by the time distribution of the observations. **When assimilating reflectance data, the ensemble needs to sufficiently spread (from an extended period without precipitation) to observe an impact of the assimilation (Fig 3a).** Inversely, and even if that may be very small, every SD observations assimilation reduces the SD ensemble independently of the precipitation events (Fig S7b, excepted for thin snow cover).

72. P. 6852, Line 25: Suggest changing “punctual usage in time” to “low temporal frequency”
Done

73. P. 6852, Line 3: It would be nice to also have an additional supplemental figure showing the impact of including both snow depth and reflectance for the 2010/11 season.

This figure was added in the supplement part (Fig S8).

We modified accordingly the section 6.4 “combining reflectance and snow depth assimilation” (See review 1, General Comment 1) as well as the Table 2 (See Review1, table and figure comments)

74. P. 6853, Line 15: Could the use of a high spatial resolution make assimilation more useful?
Yes indeed.

-----NEW-----

However, given the strong spatial variability of the snow cover, the spatial representativity of **punctual SD** measurements may make their assimilation questionable. This issue should be addressed with experiments over two-dimensional, realistic domains.

75. P. 6854, Line 7: Change “improves” to “reduces”

Done

76. P. 6854, Line 15: Change “provides results almost as good” to “reduces RMSE almost as much as”

Done

77. Table 1: Suggest changing “Standard Deviations” to “RMSE” for consistency with other parts of the paper.

See review 2, specific comments 13

78. Table 1, caption: Mention the range of years for the 18 years of observations from CdP.

-----NEW-----

Means and standard deviations (std) of the differences between SAFRAN reanalysis and `\textit{in-situ}` observations (left) and the differences between SAFRAN reanalysis and the ensemble built up in the present study (right), for the perturbed meteorological forcings. The first set of statistics is derived from 18 years (**1993-2011**) of observations and reanalysis at the CdP and the second set is derived from our 300-members ensemble over the 2010/2011 hydrological season.

Done

79. Table 2: I think having names for simulations would be more useful than including figure numbers here, or both names and figure numbers could be included. Simulations could be given meaningful names, or referred to as “case (i)”, etc. as discussed in the text.

See review2 specific comment 67

80. Table 2, caption: What does “Seasonal” refer to? The 2010/2011 season, or the period when snow cover exists for all seasons?

-----NEW-----

SD and SWE seasonal averaged RMSE computed with respect to the synthetic truth for all experiments over the 2010/2011 season. Results reported in Fig. \ref{RMSE_5seasons} are the RMSE computed over the 5 selected seasons.

81. Figure 1, caption: Change “band 1 of MODIS” to “center of band 1 of MODIS” for clarity. Define SD and SWE.

Done

82. Figure 3, caption: Change “patterns” to “shading”, when describing the envelope colors. Clarify whether the quantiles are for the baseline experiment or ensemble without assimilation.

Done

83. Figure 5: The figure is initially difficult to understand. “Model control” should be replaced by “Synthetic true snow depth”. Change the left and right titles to “SD and SD RMSE (m)” and “SWE and SWE RMSE (kg m⁻²)” for clarity.

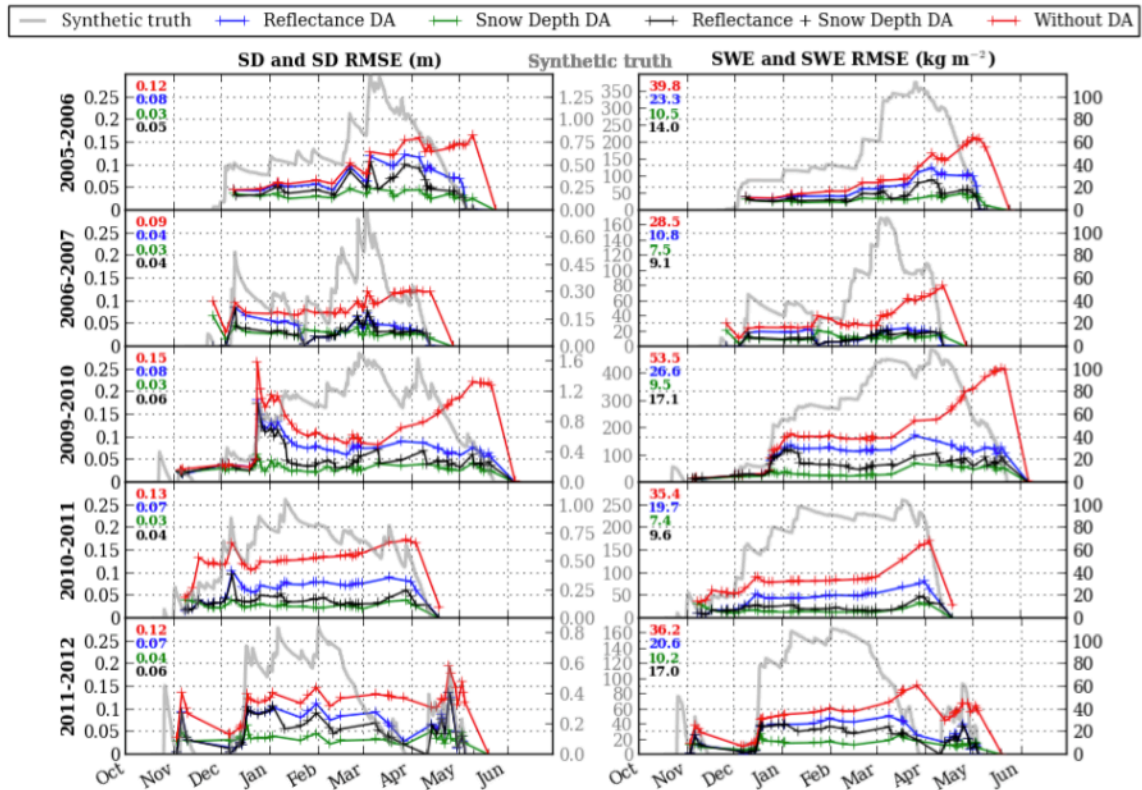


Figure 5. Time evolution of ensemble RMSEs on SD (left) and SWE (right) for the five seasons under study, for the run without assimilation (red lines), the baseline experiment (assimilating reflectances, blue lines), the experiment assimilating SD data (green lines) and the experiment assimilating combined reflectances and SD data (black lines). Crosses indicate analysis steps. Seasonal averages are displayed in the upper left corner of each graph. The model control simulation is represented by the grey lines, scaled by the "Synthetic truth" y-axes.

84. Figure 5, caption: Define "seasonal means".

Done

Seasonal averages

Technical Corrections:

All these technical corrections have been accounted for and included in the new version of the manuscript. Thank you for the very detailed proofreading.

1. Change "envelop" and "envelops" to "envelope" and "envelopes" throughout.
2. P. 6832, Line 3: Change "active microwave" to "active microwave measurements"
3. P. 6832, Line 13: Change "on board TERRA..." to "onboard the TERRA..."

4. P. 6832, Line 28: Change “snow simulations” to “snow simulation”
5. P. 6833, Line 2: Change “Moreover, 2...” to “Two...”
6. P. 6833, Line 3: Change “serie” to “series”
7. P. 6833, Line 4: Change “Indeed, the Col de Porte...” to “The Col de Porte...”
8. P. 6833, Line 6: Change “statistic” to “statistics”
9. P. 6834, Line 8: Change “of the avalanche” to “of avalanche”
10. P. 6835, Line 5: Change “its maximum” to “a maximum”
11. P. 6837, Line 15: Change “other physical laws parametrization” to “other parameterizations of physical laws”
12. P. 6837, Line 20: I believe “present section” should be changed to “following section”.
13. P. 6839, Line 2: The exponent in the expression for ϕ should be raised.
14. P. 6839, Line 10: Change “longwave radiations” to “longwave radiation”.
15. P. 6839, Line 13: Change “a week period” to “a one week period”.
16. P. 6840, Lines 2 and 3: Change “longwave radiations” to “longwave radiation”.
17. P. 6840, Line 11: Change “inter-variables” to “inter-variable”
18. P. 6840, Line 14: Change “Real data assimilation...” to “A real data assimilation...”
19. P. 6840, Line 19: Change “is not” to “are not”
20. P. 6840, Line 20: Change “their dry” to “the dry”
21. P. 6841, Line 17: Change “24 days spread” to “a 24 day spread”
22. P. 6842, Line 4: Change “ensemble of simulation” to “ensemble”
23. P. 6842, Line 21: The word “consequently” can be removed.
24. P. 6842, Line 22: Remove “In that purpose,”
25. P. 6843, Line 2: Change “than the CdL” to “as the CdL”
26. P. 6843, Line 7: Change “perturbations calibration” to “calibration of perturbations”
27. P. 6843, Line 9: Change “measurements sites” to “measurement sites”
28. P. 6843, Line 10: Change “model error” to “model errors”
29. P. 6843, Line 13: Add comma after “not crucial for our study”
30. P. 6843, Line 16: Change “prior” to “prior to”
31. P. 6843, Line 18: Change “observations datasets” to “observational datasets”
32. P. 6844, Line 1: Change “obtained” to “obtained by”
33. P. 6844, Line 12: Change “RMSE” to “RMSEs”
34. P. 6844, Line 20: Change “they are mainly varying” to “they mainly vary”
35. P. 6845, Line 4: Change “measurements provides” to “measurements provide”
36. P. 6845, Line 6: Change “later” to “latter”
37. P. 6845, Line 13: Change “to 0.003 m” to “to be 0.003 m”
38. P. 6846, Line 1: Change “simplest” to “simpler”.
39. P. 6846, Line 12: Suggest changing “particular flavor of the particle filter” to “particular type of particle filter”
40. P. 6846, Line 19: Change “distances to” to “distances from”
41. P. 6846, Line 27: Change “or” to “and”.
42. P. 6847, Line 13: Change “All along the season” to “Throughout the season”
43. P. 6847, Line 25: Change “RSME SD” to “RMSE for SD”

44. P. 6848, Line 8: Change “poorly” to “not very”
45. P. 6848, Line 17: Change “On top of this” to “Moreover”
46. P. 6848, Line 22: Remove “the” before dates.
47. P. 6848, Line 27: Change “coarsely” to “roughly”
48. P. 6848, Line 2: Change “meets limitations” to “exhibits limitations”
49. P. 6849, Line 6: Change “clouds coverage” to “cloud coverage”
50. P. 6849, Lines 12-13: Change “patterns” to “shading”
51. P. 6849, Line 18: Change “uncertainties” to “uncertainty”
52. P. 6849, Line 24: Change “are not” to “is not”
53. P. 6850, Line 9: Change “precipitations” to “precipitation”
54. P. 6850, Line 10: Change “snowfalls” to “snowfall events”
55. P. 6850, Line 13: Change “the snow melt” to “the snow melt period”
56. P. 6850, Line 24: Change “stays to 23 days” to “stays at 23 days”
57. P. 6851, Line 20: Change “all along” to “throughout”
58. P. 6852, Line 12: Change “Excepted” to “Except”
59. P. 6852, Line 16: Change “a ‘surface’ information only” to “ ‘surface’ information only”
60. P. 6852, Line 20: Change “spatialized” to “spatially distributed”
61. P. 6853, Line 13: Change “encourage to combine” to “indicate the usefulness of combining”
62. P. 6853, Line 22: Change “estimate uncertainties” to “uncertainty estimates”
63. P. 6854, Line 26: Change “kind of data assimilation” to “kinds of data assimilation”
64. P. 6855, Line 12: I believe all equations in this section should be given a number.
65. P. 6855, Line 13: I believe these equations come primarily from Gordon et al. (1993) and this reference should be referred to here.
66. P. 6856, Line 4: I believe X_{k-1} just to the right of the integration sign should be X_k
67. P. 6856, Line 5: Change “Bayes’rule” to “Bayes’ rule”
68. P. 6857, Line 8: Please provide a reference for “Kitagawa”.

On the assimilation of optical reflectances and snow depth observations into a detailed snowpack model

Luc Charrois^{1,2}, Emmanuel Cosme¹, Marie Dumont², Matthieu Lafaysse²,
Samuel Morin², Quentin Libois¹, and Ghislain Picard¹

¹Université Grenoble Alpes-CNRS, LGGE, UMR 5183, Grenoble, France

²Météo-France / CNRS, CNRM-GAME UMR 3589, CEN, St. Martin d'Hères, France

Correspondence to: Luc Charrois (luc.charrois@meteo.fr)

Abstract.

This paper examines the ability of optical reflectance data assimilation to improve snow depth and snow water equivalent simulations from a chain of models with the SAFRAN meteorological model driving the detailed multilayer snowpack model Crocus now including a two-stream radiative transfer model for snow, TARTES. The direct use of reflectance data, allowed by TARTES, instead of higher level snow products, **mitigates** uncertainties due to commonly used retrieval algorithms.

Data assimilation is performed with an ensemble-based method, the Sequential Importance Resampling Particle filter, to represent simulation uncertainties. **In snowpack modeling, uncertainties of simulations are primarily assigned to meteorological forcings. Here, a method of stochastic perturbation based on an autoregressive model is implemented to explicitly simulate the consequences of these uncertainties on the snowpack estimates.**

Through twin experiments, the assimilation of synthetic spectral reflectances matching the MODerate resolution Imaging Spectroradiometer (MODIS) spectral bands is examined over five seasons at the Col du Lautaret, located in the French Alps. Overall, the assimilation of MODIS-like data reduces by 45% the root mean square errors (RMSE) on snow depth and snow water equivalent. At this study site, the lack of MODIS data on cloudy days does not affect the assimilation performance significantly. The combined assimilation of MODIS-like reflectances and a few snow depth measurements throughout the 2010/2011 season further reduces RMSEs by roughly 70%. This work suggests that the assimilation of optical reflectances has the potential to become an essential component of spatialized snowpack simulation and forecast systems. The assimilation of real MODIS data will be investigated in future works.

1 Introduction

Seasonal snowpack modeling is a crucial issue for a large range of applications, including the forecast of natural hazards such as avalanches or floods, or the study of climate change (e.g. Durand

et al., 1999; Lehning et al., 2006; Bavay et al., 2013). The most sophisticated detailed snowpack models represent the evolution of snow microstructure and the layering of snow physical properties (Brun et al., 1989, 1992; Jordan, 1991; Bartelt and Lehning, 2002; Vionnet et al., 2012) in response to meteorological conditions. Despite constant efforts to improve these models, large uncertainties remain in the representation of the snow physics, as well as in the meteorological forcings (Carpenter and Georgakakos, 2004; Essery et al., 2013; Raleigh et al., 2015). These uncertainties are highly amplified when propagated to avalanche hazard models (Vernay et al., 2015). For operational applications, the assimilation of observations can help reduce the impact of the model and forcing uncertainties in the snowpack simulations (e.g. Dechant and Moradkhani, 2011).

Satellite observations are becoming an essential component of snow modeling and forecasting systems. *In situ* measurements are the most detailed and accurate observations of the snowpack, but their spatial distribution is far too scarce to capture the high spatial variability of the seasonal snowpack properties and improve snowpack simulations through their assimilation. For this reason, the assimilation of satellite observations of snow is an active area of research.

Snow remote sensing is primarily performed in the microwave (passive and active), visible and near-infrared spectra. Since the direct assimilation of such data requires the use of radiative transfer models, a common and simple approach consists in using satellite-based snow products. In particular, the assimilation of snow cover fraction (SCF) estimates derived from optical sensors (such as MODIS) and Snow Water Equivalent (SWE) or Snow Depth (SD) estimates derived from passive microwave sensors (such as AMSR-E) has been investigated extensively (Sun et al., 2004; Andreadis and Lettenmaier, 2006; Clark et al., 2006; Dong et al., 2007; De Lannoy et al., 2012; Liu et al., 2013).

These studies have suggested that, most of the time, assimilating snow observations may be useful to improve snowpack estimation. SWE or SD assimilation generally outperforms the assimilation of SCF only, except from (Andreadis and Lettenmaier, 2006) because of large errors in the AMSR-E SWE products. The assimilation of both combined revealed larger benefit by mitigating sensors limitations. Recently, Navari et al. (2016) investigated the assimilation of (synthetic) ice surface temperature while Dumont et al. (2012) also experimented the assimilation of albedo retrievals, both from optical sensors. Dumont et al. (2012) obtained a mass balance RMSE decrease of up to 40% assimilating albedo data. However, satellite snow products are derived using retrieval algorithms which are not perfect and, perhaps more importantly, not physically consistent with the snowpack model used for the data assimilation. For this reason, and as advocated by Durand et al. (2009) who tested the assimilation of in situ microwave radiance observations, assimilating the original satellite radiance data should be preferred when possible.

The potential of assimilating passive microwave radiances (in the form of brightness temperature) collected by AMSR-E satellite have been examined by Dechant and Moradkhani (2011)

and Che et al. (2014). Significant improvements in the SWE/SD predictions occurred but only during the accumulation period. Though the melt period, when the snowpack is wet, liquid water alters the microwave signal resulting in a lower performance of the assimilation. Moreover, for small-scale applications in mountainous areas, the coarse spatial resolution of these data considerably reduces their usefulness (Foster et al., 2005; Cordisco et al., 2006; Dong et al., 2007; Tedesco et al., 2010). As for active microwave measurements, several tests have been conducted to assimilate the satellite signal (e.g. Stankov et al., 2008; Phan et al., 2014). These tests were however limited by the accuracy of the forward electromagnetic models and by the current lack of satellite data at a daily or even weekly time frequency.

Visible and near-infrared reflectances from satellite observations have never been assimilated into snowpack models despite their great sensitivity to the snowpack properties (Warren, 1982). Even if cloud cover might limit their utility, medium and high spatial resolution data are available at daily resolution from several optical sensors (e.g. **MODerate resolution Imaging Spectrometer**, Visible Infrared Imaging Radiometer Suite) and seem to be quite suitable for complex topography (Sirguey et al., 2009). In particular, the MODIS sensor, onboard TERRA and AQUA satellites, offers a daily coverage and provides reflectance measurements in seven bands distributed in the visible (at 250 to 500 m spatial resolution), near and short-wave infrared wavelengths. Surface bi-hemispherical reflectances corrected from complex topographic effects in mountainous areas can be computed (Sirguey et al., 2009) and have been evaluated and used in several rugged areas (Dumont et al., 2012; Brun et al., 2015).

The work presented in this article examines the possibility, the relevance and the limitations of assimilating visible and near-infrared satellite reflectances into a multilayer snowpack model. A convenient approach, known as twin experiment, uses synthetic data in the same spectral bands than the real data, to examine the content of information of the observations, and the impacts we can expect from their assimilation. In twin experiments, the model used to create the synthetic data is the same as the model used for the assimilation. The synthetic observations are extracted from a member of the ensemble considered as the true state. Twin experiments are preferred in this first study in order to focus on the information content of the observations and to avoid the problem of observational biases. Data assimilation is performed with a particle filter and a Sequential Importance Resampling (SIR) algorithm (Gordon et al., 1993; Van Leeuwen, 2009, 2014). The particle filter is easy to implement, free of hypotheses about the nature of the model and the observations, and provides uncertainties in the estimation of the snowpack state.

For a comprehensive snow simulation evaluation, as recommended by Essery et al. (2013), our study is based on 5 hydrological seasons (2005/2006, 2006/2007, 2009/2010, 2010/2011, 2011/2012) which represent a wide range of possible snow cover conditions in the Alpine area. Moreover, two experimental sites were used in this work in virtue of a long, continuous time series of meteorological data and an area suitable to remote sensing measurements. The Col de Porte (CdP) area, located

100 in the Chartreuse area, near Grenoble, France (1325 m a.s.l.) provides a data set from 1993 to present (Morin et al., 2012) from which meteorological statistics can be estimated, but the instrumentation and surrounding forest at this site may affect satellite measurements. For this reason, assimilation experiments are carried out at the Col du Lautaret (CdL) located (2058 m a.s.l.) in the Ecrins area, France, which exhibits a large flat open area, above treeline, more suitable for remote sensing. **Con-**
105 **sequently, an ensemble of perturbed forcing was generated in order to represent the range of possible weather conditions at the CdL area. To this end, we developed a stochastic method using a first-order autoregressive model based on the estimated meteorological uncertainty.**

In Section 2, the SURFEX/ISBA - Crocus snowpack model used in this study is described with an emphasis on the characteristics that affect the implementation of the data assimilation method.
110 In particular, we consider the meteorological forcings as the only source of uncertainties. Section 3 presents in details how these forcings are perturbed to take the uncertainties into account in the design of the ensemble simulations. The experimental setup and the data assimilation implementation are presented in Section 4. The results of the reference assimilation experiment (baseline experiment) using **synthetic reflectance observations** at one point are presented and discussed in Section 5.
115 In close relation to this reference experiment, results of different sensitivity tests are addressed in Section 6.

2 SURFEX/ISBA - Crocus

2.1 A brief overview

The unidimensional detailed multilayer snowpack model Crocus (Brun et al., 1989, 1992) simulates
120 the evolution of the snowpack physical and microstructural properties driven by near-surface meteorology and includes a representation of snow metamorphism. A detailed description of Crocus is provided by Vionnet et al. (2012); here we only emphasize aspects that are key to data assimilation. The snowpack is vertically discretized into snow layers with different physical properties and a dynamical layering scheme handles its evolution (see details in Section 2.2). The evolution of the
125 snow cover is a function of energy and mass transfer between the snowpack and the atmosphere and the ground. The model simulates the major physical processes of snowpack evolution such as heat conduction, light penetration, water percolation and refreezing, settlement and snow metamorphism.

Crocus has been run operationally at Météo-France in support of avalanche risk forecasting over the last 20 years (Durand et al., 1999). It has been also successfully used for various applications
130 such as climate studies or hydrology (e.g. Etchevers et al., 2001; Castebrunet et al., 2014). Recently, Crocus has been integrated into the SURFEX externalized surface modeling system (Masson et al., 2013) as one of the snow schemes within the Interactions between Soil, Biosphere and Atmosphere (ISBA) land surface model (Noilhan and Planton, 1989). Thus the integrated system simulates the

energy fluxes between the snow cover and the multilayer soil component of the land surface model
135 (ISBA-DIF, Boone and Etchevers (2001)).

2.2 Layering

In Crocus, the snowpack is vertically discretized in order to realistically simulate the time evolution
of a stratified snowpack. The layering scheme is dynamical so as to preserve snowpack history and
maintain the possible thin and weak snow layers within the snowpack. The number of layers ranges
140 from 0 (bare soil) to a maximum of 50, typically. Layering is updated at the beginning of each time
step. It consists in adding, removing, or merging layers depending on their physical properties and
thicknesses. The procedure basically follows this set of rules:

- **For a snowfall on an existing snowpack, fresh snow is incorporated into the top layer if
145 (i) snow microstructure characteristics are similar, (ii) the top layer is thinner than 1 cm
and (iii) the snowfall intensity is inferior to $0.03 \text{ kg m}^{-2} \text{ h}^{-1}$. If one of these criteria is
not met or change during the time step, a new top layer is created.**
- A snowfall on bare soil forms a snowpack with a set of identical layers, the number of which
depends on the quantity of fallen snow.
- In absence of snowfall, the model seeks first to merge two thin and adjacent layers with simi-
150 lar microstructure characteristics, or inversely, split the thick ones. When the number of layers
has reached a maximum of 50, layers that are too small relative to a prescribed optimal ver-
tical profile are aggregated with adjacent ones. **This idealized thickness profile depends on
the current snow depth and on the user-defined maximal number of layers. To reach
the optimal vertical profile, the model first seeks to thin the top layers, most subject to
155 the exchange of energy, and then to keep an appropriate thickness ratio between adja-
cent snow layers to prevent numerical instabilities in the resolution of the heat diffusion
equation through the snowpack.**
- Most of the time, compaction makes layers thinner without grid resizing.

Dynamical layering adds an extra challenge in the assimilation of observations with Crocus. Data
160 assimilation methods commonly used in geophysics are well designed for fixed-grid models. For ex-
ample, the Ensemble Kalman filter involves the averaging of different snow profiles. This specificity
of Crocus largely determines our data assimilation method, as it will be discussed in Section 4.3.

2.3 Penetration of solar light in the snowpack

**Given that satellite observations indirectly relate to the quantities of interest, an observation
165 operator is required to link the satellite observation and the model state variables (Reichle,**

2008). This operator transforms the model variables into diagnostic variables to allow a direct comparison with satellite observations, preserving the physical consistency of the satellite signal with the snow model.

To this end, a new radiative transfer model was recently implemented in Crocus to calculate spectral reflectances that can be used for the comparison and the assimilation of satellite data such as MODIS. This model, named TARTES (Two-streAm Radiative TransfEr in Snow, Libois et al., 2013, 2014), simulates the absorption of solar radiation within the stratified snowpack using the δ -Eddington approximation, with a spectral resolution of 20nm. This contrasts with the original version of Crocus, where albedo was computed for three large spectral bands only and from the properties of the first two layers (Brun et al., 1992; Vionnet et al., 2012).

TARTES is implemented as an optional module to be called instead of the original Crocus albedo scheme. This implementation has no significant impact on the model structure but increases the computation time of roughly a factor 10 depending on the number of snow layers and the snow depth. TARTES makes use of four Crocus prognostic variables (specific surface area – SSA, density, snow layer thickness, impurity content and shape parameters) and the angular and spectral characteristics of the incident radiance (e.g. the solar zenith angle and the presence of cloud cover). The computation of SSA has recently been implemented by Carmagnola et al. (2014).

The use of a full radiative transfer model embedded within the snowpack model enables the assimilation of the satellite reflectance data, therefore avoiding the introduction of uncertainties from an external retrieval algorithm. And beyond its use for the assimilation of reflectances, TARTES also provides a more accurate calculation of light absorption parameters, leading to better simulations of the snowpack.

2.4 Snow impurities

Snow surface reflectance in the visible spectrum depends on the content of light-absorbing impurities in the snowpack (Warren, 1982). The impurity content can have a major impact on the snowpack simulations (Dumont et al., 2014). Despite efforts to improve the knowledge and the modeling of impurities in snow (e.g Warren and Clarke, 1990; Domine et al., 2004; Painter et al., 2007; Doherty et al., 2013), snow impurity deposition and evolution remain poorly quantified.

Currently implemented in a version of SURFEX/ISBA - Crocus, the radiative model TARTES (introduced in Section 2.3) calculates the impurity content as an equivalent black carbon content (Doherty et al., 2013; Gabbi et al., 2015). This impurity content evolves according to (i) the impurity content in fresh snow, c_0 , (ii) the time of exposure of the layer at the surface and (iii) the dry deposition flux of impurity, τ_{dry} as described in the equation below.

$$c(t + \Delta t) = c(t) + \Delta t \tau_{dry} e^{-D/h_{ref}} \quad (1)$$

where $c(t)$ is the impurity content at time t , D is the depth of the middle of the considered snow layer and $h_{\text{ref}} = 5$ cm is the e-folding of the exponential decay rate for the deposition of snow impurities ensuring that only the top layers are influenced by dry deposition.

2.5 Atmospheric forcings

205 The snowpack evolution strongly depends on near-surface meteorological forcings. These forcings are provided by the meteorological downscaling and analysis tool SAFRAN (**Systeme d'Analyse Fournissant des Renseignements Atmospheriques à la Neige; Durand et al., 1993**). SAFRAN is used to drive snowpack simulations in the French mountains because it is designed to operate at the geographical scale of meteorologically homogeneous mountain ranges, varying from 400 to
210 2000 k m². **The model combines vertical profile estimates from the ERA-40 re-analysis with observed weather data from the automatic surface observations network at different elevations, the French Snow/Weather network, rain radars, and rain gauges.** As outputs, SAFRAN provides meteorological data to the snowpack model with an hourly time step for all slopes and aspects, and a 300 m-elevation step.

215 3 Design of Crocus ensemble simulations

3.1 General strategy

In view of assimilating observations to reduce snowpack simulation uncertainties, **we first need to represent them.** As shown in Raleigh et al. (2015), the meteorological forcings are the major source of uncertainty in snowpack simulations (when a meteorological model is used to drive the snow
220 model). In the present study, air temperature, wind speed, snowfall and rainfall rates, shortwave and longwave radiative fluxes, and the deposition rate of impurities will thus be considered as the only sources of uncertainty. Snowpack model errors introduced by metamorphism and other parameterizations of physical laws are not taken into account here. **The characterization and representation of these errors, notably in the perspective of real data assimilation, will be addressed in a future
225 and dedicated work. An identified option is to use multi-physics ensemble simulations.**

We implement an ensemble method to represent the uncertainties in the forcings and their impact on snowpack simulations. An ensemble of possible realizations of the atmospheric forcings is formed and used to compute an ensemble of snow profiles representing the probability distribution of the model simulation. The following section describes the construction of the ensemble of mete-
230 orological forcings and the response of the model to this source of uncertainty, without assimilation.

3.2 Quantification of meteorological forcing uncertainties

To quantify and calibrate the meteorological forcing uncertainties, we compare 18 years of surface meteorology from SAFRAN reanalysis with *in-situ* observations at the CdP site. A long time-series

from 1993 to present (Morin et al., 2012) being available at this site, uncertainties in the SAFRAN
235 meteorological reanalysis can be estimated.

Table 1 (left column) reports the bias and the standard deviation of the difference between SAFRAN
and the observations carried out at the CdP site, for each meteorological variable (**values in brack-**
ets and the right column reports other data discussed later). The table reflects differences between
SAFRAN and *in-situ* observations, resulting, from the different spatial representativities of both
240 sources, the intrinsic errors of the analysis system **and measurement errors**.

As highlighted by Quintana Segui et al. (2008) who conducted an extended evaluation of SAFRAN
reanalysis but over a shorter period (one year), the large discrepancies between the model and the
observations can be explained by local effects due to orography and vegetation and, for the pre-
cipitation and wind speed, by the time interpolation necessary to obtain hourly forcing fields from
245 the daily analysis. For example, the precipitation analysis is performed on a daily basis in order to
include in the analysis the numerous rain gauges observations. **Radiation fluxes uncertainty might
be attributed to biases in cloud coverage and altitude estimates, effects of vegetation and sur-
rounding slopes that are not taken into account for longwave estimates. Finally, the shading
mask for shortwave radiation does not account for vegetation evolution that can also lead to
250 shortwave flux discrepancies.** Durand et al. (2009) carried out, only on a limited set of variables, a
more systematic evaluation of SAFRAN for the 1958-2002 period using 43 sites in the French Alps.
**Averaged over all locations, the RMSE on air temperature are similar to the one computed in
our study. However, their results also highlight the spatial variability of SAFRAN performance
(site RMSE ranges from -0.8 to +1.5 °C). Nevertheless, this will not have a strong impact in this
255 study since it is based on twin experiments.**

3.3 Building the ensemble of meteorological forcings

The sample of meteorological forcings is formed by perturbing the original SAFRAN reanaly-
sis with a random noise commensurate with the actual uncertainty. We thus build an ensemble
of meteorological forcings with a negligible bias with respect to the SAFRAN reanalysis and a
260 standard deviation close to the one computed from CdP statistics (Table 1, left column).

To keep the procedure simple and preserve physically consistent time variations of the forc-
ings, the random perturbations are computed using a first-order autoregressive -AR(1)- model
(Deodatis and Shinozuka, 1988) for each variable:

$$X_t = \varphi X_{t-1} + \epsilon_t, \tag{2}$$

265 with X being the perturbation value at time t and $t - 1$. φ is the AR(1) model parameter
and can be written $\varphi = e^{-\frac{\Delta t}{\tau}}$, Δt being the time step and τ the decorrelation time. Parameter

τ is adjusted for each variable, so that the perturbed variable exhibits the same frequency of temporal variations than the original variable (Fig. S1 bottom, in blue).

The amplitudes of the meteorological uncertainties are introduced with ε_t , a white noise process with zero mean and constant variance σ^2 . Variance σ^2 is computed from each standard deviation of the residuals between the reanalysis and observations at CdP (σ_{CdP} : Table 1, left column) following this equation:

$$\sigma^2 = \sigma_{CdP} \times (1 - \varphi^2) \quad (3)$$

Finally, for each meteorological variable, the selection of an additive or multiplicative perturbation method is driven by (i) the nature of the variable (ii) the dependency of the model-measurement difference to the measured values as detailed below.

For precipitation rates, shortwave radiation and wind speed, the choice of a multiplicative method is motivated by the following reasons:

- SAFRAN reanalysis captures well the occurrence of precipitation (since it assimilates surface observation network) but are more subject to errors in the amount of precipitation;
- Regarding shortwave flux and wind speed, the model biases exhibit a linear dependency to the value of the variable (not shown). Consequently, a multiplicative method was selected.

For longwave radiation and air temperature, given that there is no dependency between the model biases and the field values, an addition method is chosen.

At every time step the perturbation X_t is applied as follows:

For the additive method, $variable_t = variable_t + X_t$; For the multiplicative method, the perturbation is centered on 1 (Y_t) before multiplying the variable.

$$Y_t = X_t + 1$$

$$variable_t = variable_t \times Y_t$$

For the multiplicative method, the perturbations are bounded by 0.5 and 1.5 to avoid extreme values. The result from this perturbation method is illustrated by Fig. S1 which shows the snowfall rates over a one week period, as described by SAFRAN reanalysis, a realization of the perturbed analysis, and the full ensemble of perturbed analysis.

To maintain further physical consistency between the meteorological variables, snowfall is changed to rainfall if air temperature is higher than 274.5 °K and the shortwave radiation is

300 bounded to 200 W m^{-2} in case of rain or snow fall due to the inherent cloud cover. This behavior is consistent with the CdP statistics where over 18 years, during a precipitation period, the measured in situ shortwave radiation rarely exceeds 200 W m^{-2} .

Ensembles are generated with model errors coming from the statistics of the CdP site but as explained previously, the assimilation framework is based on the CdL area. Some adjustments
305 in the building of ensembles are also required to account differences between these two areas.

In particular, the forest at CdP affects the local wind field and the radiative fluxes (Morin et al., 2012), what explains a large part of the variability of SAFRAN errors at CdP. At CdL, an open meadow area, such variability is unlikely. To limit the overspreading of the forcing ensemble, the standard deviation used in the equation 3 for wind speed, short and longwave
310 radiation are reduced to 0.6 m s^{-2} , 70 and 7 W m^{-2} , respectively, against 1.12 m s^{-2} , 79 and 24.5 W m^{-2} (Table 1, left column, values in brackets). As shown in Table 1, the standard deviations computed from the generated ensemble (right column) are close to the ones prescribed to generate it (left column).

In the end, this stochastic method of perturbations makes possible the construction of an
315 ensemble of perturbed forcings which are required when using ensemble methods. The calibration of the perturbations are based on the CdP statistics while their temporal correlation is ensured by the AR(1) model. The perturbation method exhibits some obvious limitations. Inter-variable correlations are indeed not taken into account in the ensemble except from the precipitation phase and the maximum value of shortwave radiation in case of precipitation.
320 Adjustments to CdL are somewhat subjective, but this is not crucial in our twin experiment context since the considered truth will be simulated running Crocus with one forcing member drawn from this generated ensemble. A more physically consistent ensemble will be required when real data assimilation is investigated.

3.4 Perturbation of impurity deposition rate

325 In this study, the deposition fluxes of impurities are also considered as a meteorological forcing but unlike meteorological variables previously mentioned (Section 2.5), the deposition fluxes of impurities are not provided by the SAFRAN model. Instead, the impurity content in fresh snow c_0 and the dry deposition flux τ_{dry} are perturbed online during a model run.

The parameters c_0 and τ_{dry} are subject to multiplicative perturbations drawn from lognormal
330 distributions. The perturbations are constant in time, but are reinitialized at each observational update when data assimilation is performed. For c_0 , the probability density function (pdf) parameters are $\sigma=0.8$ and $\mu=0$. c_0 is bounded at 0 and 500 ng g^{-1} and the mode value of the pdf is 100 ng g^{-1} . As for τ_{dry} , the pdf parameters are $\sigma=1.2$ and $\mu=0$. τ_{dry} is bounded at 0 and $0.5 \text{ ng g}^{-1}\text{s}^{-1}$ with a mode value of $0.015 \text{ ng g}^{-1}\text{s}^{-1}$. These values have been selected to obtain the same order of magnitude
335 of albedo decrease with snow age as in the original Crocus formulation (Brun et al., 1992).

3.5 Ensemble simulations

To investigate the impact of the stochastic perturbations, an ensemble of 300 simulations of the snowpack, forced by the 300 forcings of the meteorological ensemble, is run over the 2010/2011 hydrological season without data assimilation. **Figure 1 presents the result of the ensemble simulation with 300 members (represented by the black lines).** The simulation forced by the unperturbed reanalysis (red line) is included within the envelope of the ensemble. The spread of the ensemble reflects the consequences of possible overestimations and underestimations of meteorological data by the reanalysis.

The spread of the SD and SWE ensembles (Fig. 1 (b)-(c)) is the largest at the end of the season, leading to a range of 24 days from the first to the last member to fully melt. The maximum dispersion range of SWE ($\Delta\text{SWE}\approx 300\text{ kg m}^{-2}$) occurs in early April. At this time, the snowpack in some ensemble members has just started to melt, while in other cases, the snowpack has already disappeared.

Snowfalls reset all members to high reflectance values (at 640-nm, 0.98 for a significant event, Fig. 1 (a)) and drastically reduce the spread of the reflectance ensemble. Concomitantly, the SD and SWE ensemble spreads can increase due to the uncertainties in the precipitation rates. After a snowfall, impurity content and grain size increase along with the age of snow, decreasing the surface reflectance. This evolution is also influenced by atmospheric forcings, which are slightly different from one ensemble member to another, enlarging the spread of the ensemble. We can therefore expect that the timing of the available reflectances will strongly affect the impact of their assimilation on the snowpack ensemble simulations.

3.6 Dispersion of the ensemble of Crocus simulations

Here we assess whether our ensemble represents a realistic spread of SD over time with respect to previous evaluations of the model through a spread-skill plot.

Given that no SD measurements were systematically carried out at the CdL site, we were not able to evaluate our ensemble spread from SAFRAN-Crocus simulations with a time series of *in-situ* measurements at this site. But, as demonstrated by Fortin et al. (2014), the ability of the ensemble spread to depict the simulation error can be evaluated by the comparison of the RMSE and the ensemble spread (Spd) with respect to the ensemble mean.

Firstly, using the method previously described, an ensemble of Crocus simulations was carried out at the CdP site, with no adjustment on CdP statistics, to evaluate the relevance of our perturbation method by comparing the RMSE between SAFRAN-Crocus simulation and in situ measurements with the Spd of the CdP ensemble. Then, we compare the Spd of our ensemble simulation at the CdL site with a SAFRAN-Crocus RMSE computed from the difference between SD Crocus estimates with in situ SD measurements across multiple stations

(at the same elevation than CdL). We used roughly 60 daily snow depth measurements stations from the Météo-France observation stations network (only stations within the same altitude range as the CdL site (1800 - 2200m a.s.l.)).

The multiple station RMSE and Spd terms are defined as follows, for a variable X ,

$$375 \quad \text{Spd}(X) = \left(\frac{1}{M} \sum_{t=1}^M \frac{1}{N_e} \sum_{n=1}^{N_e} (X_{t,n} - \bar{X}_t)^2 \right)^{1/2}, \quad (4)$$

$$\text{RMSE}(X) = \left(\frac{1}{M} \sum_{t=1}^M \frac{1}{N_k} \sum_{k=1}^{N_k} (X_{t,k}^{\text{model}} - X_{t,k}^{\text{in situ}})^2 \right)^{1/2}, \quad (5)$$

where M represents the number of time steps, N_e the size of the ensemble and N_k the number of in situ measurements. The SD value of the ensemble member n at the date t is $X_{t,n}$ and \bar{X}_t is the mean of the ensemble at the date t . The value from SAFRAN-Crocus simulation at the measurement site k and at the date t is given by $X_{t,k}^{\text{model}}$, and $X_{t,k}^{\text{in situ}}$ is the value from the in situ SD measurement. RMSE and Spd are computed at observation times. For comparisons based on only one point, the RMSE equation for a variable X becomes:

$$\text{RMSE}(X) = \left(\frac{1}{M} \sum_{t=1}^M (X_t^{\text{model}} - X_t^{\text{in situ}})^2 \right)^{1/2}, \quad (6)$$

Figure 2 (a) shows that at the CdP site the SD dispersion (Spd) of the ensemble is consistent with the RMSE between SAFRAN-Crocus simulation with respect to in situ measurements at this site. This suggests that our perturbation method is able to represent the forcing uncertainties on snowpack simulations. Nevertheless, concerning the CdL area over the 2010/2011 season, the SAFRAN-Crocus RMSE is roughly two times higher than the SD dispersion (Spd) of our ensemble (Fig. 2 (b)). This means that our ensemble is under-dispersive in terms of SD. This may be partly explained by the calibration of perturbations, based on statistics at a location (CdP) which is not highly affected by wind erosion/accumulation in contrast to many other measurement sites. In addition, only meteorological errors are considered in our ensemble whereas the other model errors also contribute to the simulation error.

Nonetheless, given that experiments in the present work are twin and that the observations are selected within the ensemble (synthetic observations), the impact of this under dispersion is not crucial, but will be considered when using real data.

4 Data assimilation setup

This section describes the assimilation framework and the assimilation strategies designed for this study prior to presenting results of assimilation experiments (Section 5 and 6). First of all, the experimental setup and diagnostics applied in this study are detailed before describing the two synthetic

observational datasets used for assimilation. An overview of the SIR filter is given at the end of this section and further details are provided in the appendix A.

4.1 General settings and diagnostics

The assimilation experiments are twin, meaning that the observations are synthetics and come from a single model simulation. They are performed over five winter seasons at the CdL area.

A synthetic truth simulation is first obtained by running Crocus, through the use of the radiative transfer model TARTES, forced by one perturbed meteorological forcing, as detailed in Section 3.3. The synthetic observations used in all the assimilation experiments reported in Sections 5 and 6 are extracted from this synthetic truth simulation. The synthetic truth simulation is also considered as the truth to evaluate the performance of data assimilation.

Data assimilation performances are evaluated by comparing RMSE for ensembles with and without assimilation, and by comparing the synthetic true simulation to the 33rd, 50th, and 67th quantiles from the ensembles with assimilation.

For a variable X , the ensemble RMSE is defined as:

$$\text{RMSE}(X) = \left(\frac{1}{N_e} \sum_{n=1}^{N_e} (X_n - X^{\text{truth}})^2 \right)^{1/2}, \quad (7)$$

where N_e represents the size of the ensemble, X_n the value from the ensemble member n , and X^{truth} the value from the synthetic truth. RMSEs are computed at observation times. The uncertainty on the melt-out date is quantified as the difference (in days) between the first and the latest full melted member.

4.2 Nature of the assimilated observations

The first set of synthetic observations is composed of surface reflectances of the first seven bands of MODIS (central wavelengths : 460, 560, 640, 860, 1240, 1640, 2120 nm; Hall and Riggs, 2007). In twin context, these synthetic observations are provided from the synthetic truth simulation running Crocus with its radiative TARTES model. Snow surface reflectances in the visible and near-infrared spectra are sensitive to the properties of the first millimeters to the first centimeters of the snowpack for a given wavelength (Li et al., 2001). They mainly vary with snow microstructure (near-infrared part) and impurity content (visible part) (Warren, 1982). The reflectance observations error variances, necessary for the assimilation, are defined according to Wright et al. (2014). They are prescribed to $7.1 \cdot 10^{-4}$, $4.6 \cdot 10^{-4}$, 5.610^{-4} , 5.610^{-4} , 2.010^{-3} , 1.510^{-3} and 7.810^{-4} , for the seven bands, respectively. In the framework of our twin experiments, the covariance matrix of observation errors is diagonal. Note that the TARTES model calculates bi-hemispherical reflectances while the satellite measurements provide directly hemispherical-conical top of atmosphere reflectances (Dumont et al., 2012).

The second set of observations is composed of **synthetic snow depth (SD) observations**. Previous studies have indeed reported that the assimilation of snowpack bulk variables such as SD greatly improve snow estimations (Morin, 2014; Liu et al., 2013). However, SD observations are only available at one point. In our study, the observation error variance of SD is taken to be 0.003 m (corresponding to a standard deviation of about 5 cm). The impact of **synthetic SD assimilation** is detailed in Section 6.3.

The setup designed in our study (one point, twin experiments) allows relevant comparisons of the benefits of assimilating separately or jointly the two above mentioned types of observations. **For future works assimilating real data, the difference in the geometrical configuration between the simulated TARTES reflectances and satellite observations will be addressed.**

4.3 Assimilation method: The particle filter

The data assimilation method has been chosen after considering the requirements and the possible degrees of freedom that our problem imposes or offers.

Firstly, we require that the method quantifies uncertainties. This plays in favor of ensemble methods (e.g. Blayo et al., 2014). Secondly, we prefer an already existing and well tested method. This argues for the Ensemble Kalman Filter (EnKF, Evensen, 2009) or the particle filter (Van Leeuwen, 2009, 2014). Thirdly, the method should not rely on assumptions about the physical system, such as linearity or weak nonlinearity, because the physics of our model are nonlinear. This draws us toward the particle filter. Fourthly, the method should be easy to implement for this first study. Abaza et al. (2015) assessed the effectiveness assimilating streamflow data using an EnKF sequential procedure but implemented in a simpler snow scheme than Crocus. The fact that the EnKF involves state-averaging operations, to which Crocus hardly complies due to its varying number of snowpack layers, argues in favor of the particle filter. Note that Dechant and Moradkhani (2011) also chose the SIR filter for the assimilation of microwave radiances in a snowpack model. The major drawback of the particle filter is that it is not applicable to high-dimensional systems (Snyder et al., 2008) because it quickly degenerates (all ensemble members converge toward a unique and spurious model trajectory). But our model, with hardly more than a few hundreds of variables, is not high-dimensional. Our experiments show it indeed does not degenerate if a well-tested resampling method is used, with ensembles of a few hundreds of members only. Thus, we choose the *Sequential Importance Resampling* (SIR) filter (Gordon et al., 1993), which is a particular type of the particle filter. Our ensembles are composed of 300 members.

The SIR filter seeks to represent the probability density function (pdf) of the model state by a discrete set (an ensemble) of states commonly called particles. The propagation over time of all particles, through the nonlinear model equations, describes the evolution of the model pdf. When observations are available, the ensemble is updated following two steps: (i) the particles are weighed according to their respective distances from the observations, and (ii) the pdf defined by the newly

470 weighted particles is resampled by ruling out particles with negligible weights, and duplicating particles with large weights, so that the updated pdf is again represented by an ensemble of equally-weighted particles. The new ensemble is then ready to be propagated in time by the model. As long as a particle is not removed, it keeps its original perturbed forcing to be propagated. **Inversely, a new perturbed forcing is assigned to a duplicated particle for propagation to the next analysis. The**
475 **governing equations of the data assimilation scheme are given in the Appendix A and more details are presented in Van Leeuwen (2009) and Van Leeuwen (2014).**

5 Assimilation of MODIS-like reflectances

In this section, we assess to what extent the assimilation of the available MODIS-like reflectance observations allows the accurate estimation of snowpack properties throughout the season. This
480 experiment will be considered as our baseline experiment.

Data assimilation results for the 640-nm and 1240-nm reflectance (first and fifth MODIS bands) and for SD and SWE over the hydrological season 2010/2011 are shown in Fig. 3. **To mimic real cloud conditions, reflectances are assimilated at 34 clear sky days of the season. We define a clear sky date according to the real cloud mask from MODIS data computed with the method**
485 **of Sirguey et al. (2009).** The corresponding 640-nm and 1240-nm **synthetic reflectance observations** are shown by the red dots in Fig. 3 (a) and (b). The control simulation (from which **the synthetic observations are drawn**) is shown by the red lines.

Throughout the season, the envelopes of SD and SWE ensembles for the baseline experiment (Fig. 3, blue envelopes) include the control simulation, which is a prerequisite for the
490 **good behavior of the assimilation.** Overall, the assimilation of reflectance observations reduces the uncertainties in the estimation of the snowpack characteristics throughout the season. This is observed in Fig. 3, where the baseline experiment envelopes (blue shading) are narrower than those of the ensemble without assimilation (grey shading). In particular, the snow melt-out date is estimated much more accurately with the assimilation of reflectances: the uncertainty range drops from 24
495 days without assimilation to 9 days with assimilation.

Figure 4 shows the time evolution of the RMSE with assimilation at every observation time, at the end of the forecast step (blue solid line) and just after the filter analysis (blue dotted line). These results are compared to the RMSE without assimilation (grey lines). The RMSE of the ensemble with assimilation is always lower than the RMSE without assimilation. **Averaged over**
500 **the season, a reduction of 46% was obtained for SD and 44% for SWE, (Table 2: seasonal RMSE for SD: 0.07 m; SWE: 19.7 kg m⁻² compared to 0.13 m and 35.4 kg m⁻² from the ensemble without assimilation).** These results indicate the usefulness of using spectral optical radiance rather than albedo data since Dumont et al. (2012) obtained an improvement in SD estimate of only 14% when assimilating albedo retrievals from MODIS sensor. It is remarkable

505 **that, despite the significant RMSE reduction in our experiment, there is most of the time no**
strong reduction of the RMSE from a single analysis. The reduced RMSEs with assimilation are
consequently due to **the successive observations throughout the season**, highlighting the role of
model dynamics.

The strongest RMSE reductions occur right after extended periods without precipitation
510 **and without available observations, when the reflectance ensemble spread is particularly pro-**
nounced (e.g. Fig. 3 (a)). During these periods (e.g. from 07/12/2010 to 14/12/2010, or from
11/01/2011 to 21/01/2011), the ensemble uncertainties on reflectances, SD and SWE grow under the
influence of the perturbed forcings including the perturbed impurity deposition rate. Observations of
reflectances have a large impact when they are used. However, since reflectance observations are not
515 very sensitive to the inner snowpack hidden by recent snowfalls, the uncertainties on SD and SWE
accumulated earlier and not corrected by past analysis remain, which ultimately results in limited
corrections on SD and SWE (Fig. 3, for example, on 28/01/2011), and sustained ensemble spreads
and RMSE throughout the season.

After a significant snowfall, the uncertainties in SD and SWE may increase, and the assimilation
520 of reflectances generally has a very small impact on these two variables. Indeed, the uncertainty
in the amount of snowfall (translated here in perturbations on the snowfall rate) tends to increase
the ensemble spread and RMSE on SD and SWE. Moreover, whether it be in the visible range
of wavelengths sensitive to the impurity content or in the infrared part where changes on the mi-
crostructure dominates, **a snowfall resets all ensemble members to the same set of reflectance**
525 **values. This makes the discrimination between members using reflectances alone impossible,**
and the subsequent analysis provides a rather small uncertainty reduction for SD and SWE.
This is illustrated on Fig. 3 on 10 November and on 1 December 2010, for example.

The remarks stated above for the season 2010/2011 hold for the other seasons. Figure 5
reports the time evolution of the SD and SWE RMSEs for all the selected seasons, in the ex-
530 **periments without assimilation (red lines) and with assimilation of reflectances (blue line; the**
experiments shown in green and black are discussed in the next section). On average, SD and
SWE RMSEs are reduced by 45% and 48%, respectively. This is comparable with results of
Che et al. (2014), who assimilate radiances in the microwave spectrum from AMSR-E, and
reduce the SD RMSE by 50%. However, passive microwave observations are very sensitive to
535 **liquid water. Consequently, the performance of the assimilation during the melting period is re-**
duced (Che et al. (2014) reduce the SD RMSE up to 61% from January to March, during only
the dry snow period). In contrast, our results show a well-marked reduction of errors near the
end of the seasons (Fig. 2, grey lines and blue dotted lines). Our results are also consistent with
those from Liu et al. (2013) assimilating MODIS-derived Snow Cover Fractions (SCF), after a
540 **processing of the retrieval to improve accuracy of cloud coverage and snow mapping. Without**

this processing, the performance of SCF assimilation falls, with a SWE RMSE reduction near 10-20%, similarly to (Andreadis and Lettenmaier, 2006).

Consequently, our ability to control the seasonal evolution of the snowpack with the assimilation of reflectances is demonstrated, though it exhibits limitations. In particular, the reduction of the snowpack SD and SWE ensemble spread greatly depends on the timing of the assimilated observations.

6 Sensitivity to the nature and the timing of observations

6.1 Impact of cloud coverage on the experiment

The presence of **cloud coverage** strongly reduces the number of optical data available for assimilation. To investigate impact of **limiting the number of available observations**, an experiment similar to the **baseline experiment** (see Section 5) is carried out, **but assimilation is performed every day**, (134 days) instead of 34 days in the baseline experiment. Figure S2 presents the results with the blue shading representing the envelopes of the ensemble assimilating daily MODIS-like observations and the grey shading the envelopes of the baseline experiment, reported from Fig. 3.

Obviously, in this second experiment, concerning the 640-nm reflectance variable, **the spread of the ensemble is greatly reduced, well fitting the observations (red dots) and its envelope does not show any extended periods with a large range of reflectance values anymore (Fig. S2 (a)).** Compared to the baseline experiment (grey envelopes), the uncertainty in the snow melt-out date is also reduced to 3 days. However during the major part of the winter, the SD and SWE ensemble spreads (Fig. S2 (b)-(c): blue envelopes) are comparable to the spreads obtained in the baseline experiment (Fig. S2 (b)-(c): grey envelopes). This is also reflected in Table 2: The seasonal RMSEs on SD and SWE are 0.05 m and 14.4 kg m⁻², respectively, against 0.07 m and 19.7 kg m⁻² in the baseline experiment. **This shows that assimilating a limited number data due to realistic cloud conditions is not necessarily harmful to the estimation of the snowpack state.** Note that this conclusion holds here for bulk variables such as SD and SWE. The estimation of other physical properties of the snowpack will be addressed in a future work using real observations.

6.2 On the timing of observations

The baseline experiment suggests that the timing of observations may largely determine the quality of the assimilation process. To explore the role of the timing, four additional assimilation tests are designed for which MODIS-like reflectances are assimilated (i) only at the beginning of the season (before 31/12/2010, **Fig. S3: Accu**), (ii) only in the second part of the snow season (after 31/12/2010, **Fig. S4: Melt**), (iii) only after several day-long periods without precipitation (**Fig. S5: Before Snowf**) and (iv) only right after snowfall events (**Fig. S6: After Snowf**).

In case **(i: Accu)**, results show that even if the SD and SWE spreads are reduced during the assimilation period, the assimilation has almost no effect on the snow estimates during the snow melt period. **The ensemble spread at the end of the season returns to almost the same value than the experiment without assimilation.** The uncertainty of the snow melt-out date is reduced to 22 days only, in comparison with 24 days without assimilation. As for case **(ii: Melt)**, the spread reduction becomes quite discernible roughly 2 months after the first assimilation date and never reaches the value of the baseline experiment. The uncertainty of the snow melt-out date is however reduced to 11 days. This demonstrates that it is essential to assimilate reflectances over the entire season to compensate the fast growth of the snowpack ensemble in response to the uncertainties in the meteorological forcing.

In both cases **(iii: Before Snowf)** and **(iv: After Snowf)**, reflectances are assimilated at only 7 dates of the season. Case **(iii: Before Snowf)** exhibits a more pronounced SD and SWE spreads reduction compared to case **(iv: After Snowf)**. The uncertainty on the snow melt-out date drops to 9 days in case **(iii: Before Snowf)** while it stays at 23 days in case **(iv: After Snowf)**. In absence of precipitation, the snow surface is aging, leading to a decrease of reflectance values and a spread of the reflectance ensemble (Fig. S5 (a)). Therefore, an observation after such a period provides a significant amount of information and produces an efficient analysis. On the contrary, solid precipitation resets the reflectance to high values and limits the spread of the reflectance ensemble (Fig. S6 (a)) leading to a limited efficiency of the ensemble analysis. Assimilating only a few **synthetic observations** well distributed in time nearly leads to the same uncertainty of SD and SWE estimates as the baseline experiment assimilating 34 observations (**Table 2 - Before Snowf:** seasonal RMSE SD: 0.07 m; SWE: 21.8 kg m⁻² compared to baseline experiment 0.07 m and 19.7 kg m⁻², respectively)

Consequently, the time distribution of the observation turns out to be a key element in the expected success of the assimilation of reflectance observations. The end of an extended period without precipitation, when the surface snow layer is aging, is the best time to assimilate reflectances.

6.3 Assimilation of snow depths

To better evaluate the impact of the reflectance assimilation, we here compare the baseline experiment to an experiment assimilating synthetic SD observations keeping the same time distribution of the observations. Apart from the different nature of the observations, the assimilation setup is the same as the one described in Section 5 including the time frequency of observations. The results are displayed in Fig. S7.

The assimilation of **synthetic SD observations** greatly improves the estimates of SD and SWE (Fig. S7 (b)-(c)). The spread reduction is much stronger than with the assimilation of reflectance observations (Table 2: the seasonal RMSE on SD and SWE are 0.03 m and 7.4 kg m⁻², respectively, against 0.07 m and 19.7 kg m⁻² in the baseline experiment) and is maintained throughout the season.

610 The uncertainty range on the snow melt-out date is decreased to 8 days compared to 9 assimilating
MODIS-like reflectances and 24 days without assimilation for the 2010/2011 season. Note that the
spread reduction of the reflectance ensemble is very limited compared to the baseline experiment.
This is consistent with the fact that while SD and SWE are better estimated in the case of SD
simulation, the surface and inner physical properties of the snowpack are less impacted than in the
615 case of assimilating reflectance observations.

Figure S7 shows that, at the beginning of the snow season (before 16/11/2010) and for a thin
snowpack (less than 20 cm), SD assimilation seems to have less impact than reflectance assimilation.
Indeed, with a thin snowpack, visible wavelengths penetrate down to the ground, and reflectance
contains information on the whole snowpack. In this case, reflectance contains more information
620 than SD. This could explain the better performance of the baseline experiment.

An additional experiment (not shown here) was also conducted assimilating daily synthetic SD
observations because such measurements are usually daily available at about 60 different stations in
the French Alps. This shows that on the contrary to reflectance assimilation, for SD assimilation, the
more frequent the observations, the greater the spread reduction (seasonal RMSE SD: 0.02 m; SWE:
625 4.7 kg m^{-2}).

Except for thin snow cover, the assimilation of SD observations outperforms reflectance assimi-
lation in terms of SWE and SD estimates and seems to be less affected by the time distribution of
the observations. **When assimilating reflectance data, the ensemble needs to sufficiently spread
(from an extended period without precipitation) to observe an impact of the assimilation (Fig.
630 3 (a)). Inversely, and even if that may be very small, every SD observations assimilation re-
duces the SD ensemble independently of the precipitation events (Fig. S7, excepted for thin
snow cover).**

Figure 5 also shows that, all these findings obtained for the 2010/2011 season are also ver-
ified for the five studied seasons. All assimilation experiments of synthetic SD observations
635 reduce the RMSE with respect to both the model run without assimilation (red lines) and the
experiments assimilation synthetic reflectances data (blue lines). However, in case of shallow
snowpack, the better performance is obtained using reflectance data.

6.4 Combining reflectance and snow depth assimilation

Though the assimilation of **synthetic** SD observations generally outperforms MODIS-like reflectance
640 assimilation, spatially distributed SD measurements are rarely available over large areas on a daily
basis. *In-situ* SD observations give information only at the measurement point and many studies
attest to the strong spatial variability of the snow cover (e.g. López-Moreno et al., 2011; Veitinger
et al., 2014; Bühler et al., 2015). Airborne LiDAR or ground based laser LiDAR provide accurate SD
measurements with fine resolution, **but their low temporal frequency limits** their utility for opera-
645 tional applications. So, one can imagine that over a mountain range, SD measurements are available

at several locations for only a few dates in the season (e.g. occasional snow course, crowd-sourcing, ski resorts observations, ...). This scenario motivates the set-up of the following experiment. The experimental setup is the same as the baseline reflectance assimilation scheme previously described with an extra **synthetic SD observation** the 10th of each month. Results **are shown in Fig. S8** and compared to the previous experiments in Fig. 5.

Combining the assimilation of MODIS-like reflectances with the assimilation of synthetic SD observations provides a benefit compared to assimilating reflectance only (Fig. 5, black and blue lines respectively). (i) In presence of a thin snow cover, the SD and SWE RMSEs of the combined reflectances and SD ensembles are reduced as the ones from the assimilation of the reflectance only. (ii) Almost all along the season, SD and SWE RMSEs remain below the reflectance assimilation RMSE thanks to SD assimilation. The combined assimilation leads to SWE seasonal RMSE of 9.6 kg m^{-2} to be compared to 7.4 kg m^{-2} for the experiment assimilating **synthetic SD observations** and 19.7 kg m^{-2} for the baseline reflectances assimilation experiment (Table 2).

These results indicate the usefulness of combining these two datasets in operational applications. Liu et al. (2013) reached a similar conclusion by combining the assimilation of SCF and SD (with an SWE RMSE reduction up to 72%; up to 74% in our study). However, given the strong spatial variability of the snow cover, the spatial representativity of punctual SD measurements may make their assimilation questionable. This issue should be addressed with experiments over two-dimensional, realistic domains.

7 Conclusions

This study investigates the assimilation of MODIS-like reflectances from visible to near-infrared (the first seven bands) into the multilayer snowpack model Crocus. The direct use of reflectance data instead of higher level snow products limits the introduction of uncertainties due to retrieval algorithms. For the assimilation, we implement a particle filter. A particle filter is chosen because (i) it is an ensemble method providing uncertainty estimates, and (ii) it is easily implemented (in comparison with other assimilation methods) with Crocus model, characterized by strong nonlinearities and its lagrangian representation of the snowpack layering. Given that the major source of error in snowpack simulations can be attributed to meteorological forcings, a stochastic perturbation method is designed to generate an ensemble of possible meteorological variables. This algorithm uses a first-order autoregressive model to account for the temporal correlations in the meteorological forcing uncertainties. This ensemble of meteorological forcings is then applied to generate the ensemble of snowpack simulations for the assimilation. Twin experiments are conducted at one point in the French Alps, the Col du Lautaret, over five hydrological years. The assimilated reflectance data corresponds to the first seven spectral bands of the MODIS sensors.

680 Reflectance assimilation using only data from clear-sky days reduces the SD and SWE seasonal
RMSE by a factor close to 2. The uncertainty range on the snow melt-out date drops to 9 days com-
pared to 24 without assimilation. Additional assimilation tests using different time distributions of
the observations show that (i) reflectance assimilation greatly improves snowpack estimates if the
observation comes after an extended period without precipitation, (ii) the assimilation has almost
685 no impact if it comes right after a snowfall, and (iii) using only a few observations with the appro-
priate timing, i.e. after extended periods without precipitation, **reduces RMSE almost as much as
assimilating** reflectances on a daily basis.

The assimilation of synthetic SD observations leads to a decrease of SD and SWE RMSE by
a factor of more than 4. The uncertainty range on the snow melt-out date is reduced to 8 days.
690 The assimilation of SD observations generally outperforms reflectance assimilation except for thin
snowpacks, typically less than 20 cm. However, whereas optical reflectance maps can be obtained
daily thanks to spaceborne sensors such as MODIS or VIIRS, SD measurements are rarely available
either over large areas or at the same time frequency. **Combining reflectance assimilation with SD
assimilation at 4 dates during the snow season leads to a decrease of SD and SWE RMSE by a
695 factor close to 3.**

This study provides a general theoretical framework to test the efficiency of several kinds of data
assimilation in a snowpack model and highlights the benefit of using remotely sensed optical surface
reflectance in the assimilation scheme to provide significant improvements of the snowpack SD and
SWE estimates. Even if the assimilation of SD outperforms the assimilation using reflectance data,
700 the sparsity of *in-situ* measurements in space and/or time strongly reduces their utility in real data
assimilation systems. Nevertheless, given their complementary features, combining remotely sensed
reflectances and SD data, when available, would definitely improve snowpack simulations.

This study presents a first attempt to assimilate snow observations into the Crocus snowpack
model with the overarching objective of improving operational snowpack forecasting. The next steps
705 to proceed toward operational applications must include the assimilation of actual satellite data and
the spatialization of the assimilation on larger domains. These steps include several challenges such
as the increased calculation costs and degrees of freedom, and the need for a physically consistent
2D meteorological ensemble, which will be addressed in future work.

Appendix A: PARTICLE FILTER AND SEQUENTIAL IMPORTANCE RESAMPLING,

710 DEFINITIONS (Gordon et al., 1993; Van Leeuwen, 2009, 2014)

In a discrete-time space model, the state of a system evolves according to:

$$x_k = f_k(x_{k-1}, v_{k-1}), \quad (\text{A1})$$

where x_k is the state vector of the system at time k , v_{k-1} is the state noise vector and f_k is the non-linear and time-dependent function describing the evolution of the state vector.

715 Information about x_k is obtained through noisy measurements, y_k , which are governed by the observation operator equation:

$$y_k = h_k(x_k, n_k), \quad (\text{A2})$$

where h_k is a possibly non-linear and time-dependent function linking the state vector to the observation (observation operator) and n_k is the measurement noise vector.

720 The filtering problem is to estimate sequentially the values of x_k , given the observed values y_0, \dots, y_k , at any time step k . In a Bayesian setting, this problem can be formalized as the computation of the distribution $p(x_k | y_{1:k})$, which can be done recursively in two steps:

Prediction step:

$$p(x_k | y_{1:k-1}) = \int p(x_{k-1} | y_{k-1}) p(x_k | x_{k-1}) dx_{k-1}. \quad (\text{A3})$$

725 Updating step to estimate $p(x_k | y_{1:k})$ using Bayes' rule:

$$p(x_k | y_{1:k}) \propto p(y_k | x_k) p(x_k | y_{1:k-1}). \quad (\text{A4})$$

In the particle filter, the prior pdf is represented by equally-weighted delta functions centered on the ensemble members or particles:

$$p(x_{k-1} | y_{1:k-1}) = \frac{1}{N} \sum_{i=1}^N \delta(x_{k-1} - x_{k-1}^i), \quad (\text{A5})$$

730 where N is the ensemble size. With this representation, the propagation step A3 provides:

$$p(x_k | y_{1:k-1}) = \frac{1}{N} \sum_{i=1}^N \delta(x_k - x_k^i), \quad (\text{A6})$$

where $x_k^i = f(x_{k-1}^i, v_{k-1}^i)$; v_{k-1}^i is a realization of the noise v_{k-1} . Then the analysis step follows with:

$$p(x_k | y_{1:k}) = \sum_{i=1}^N w_k^i \delta(x_k - x_k^i), \quad (\text{A7})$$

735 where the w_k^i are the particle weights, normalized to sum up to 1, and given by:

$$w_k^i \propto p(y_k | x_k^i). \quad (\text{A8})$$

To compute the weights, the error n_k of the observation operator h_k (Eq. A2) is often considered additive and Gaussian with mean 0 and covariance matrix R_k , so that the likelihood $p(y_k|x_k^i)$ writes:

$$740 \quad p(y_k|x_k^i) \propto \exp\left(-\frac{1}{2}(y_k - h(x_k^i))^T R^{-1}(y_k - h(x_k^i))\right). \quad (\text{A9})$$

After the computation of the weights, the ensemble is resampled: particles with zero or negligible weights are ruled out; particles with large weights are duplicated a number of times commensurate with their weights. Several algorithms exist for this resampling step; we use the one of Kitagawa (Kitagawa, 1996).

745 *Acknowledgements.* We wish to thank the two anonymous reviewers for their detailed comments. We gratefully acknowledge funding from Labex OSUG@2020 (Investissements d'avenir - ANR10 LABX56) and Fondation Eau Neige et Glace. This work has also been supported by the INSU/LEFE/MANU program. The development of the radiative model TARTES has been funded by the French ANR MONISNOW project, number ANR-11-JS56-0005.

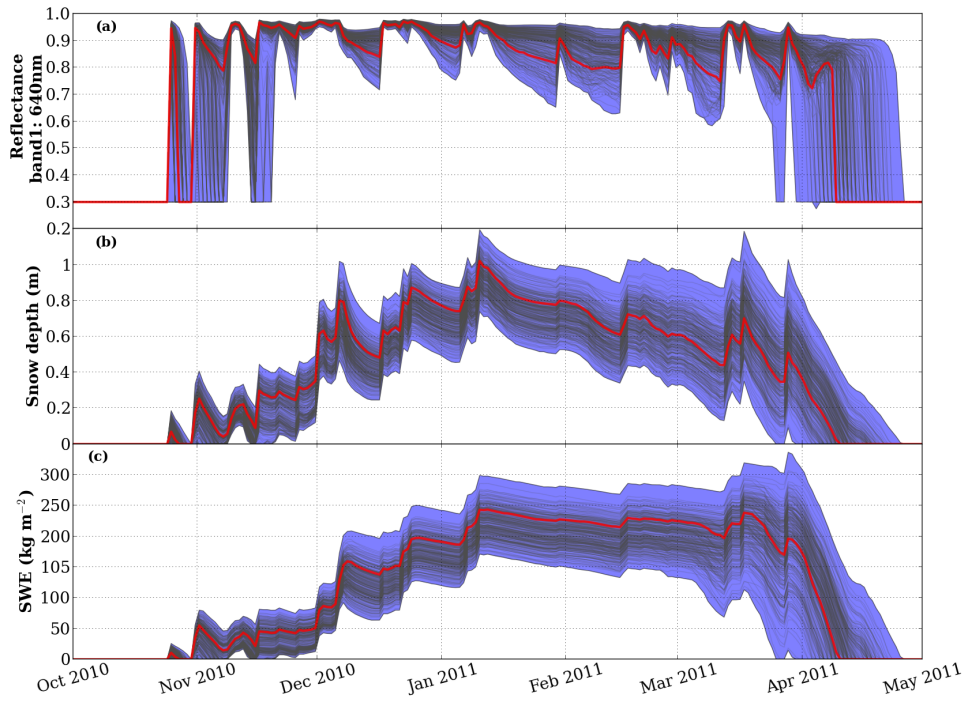


Figure 1. Ensemble simulation with 300 members at the Col du Lautaret site over the 2010/2011 hydrological season. (a) Reflectance at 640 nm (**center of band 1 of MODIS**), (b) SD, and (c) SWE. On each graph, the red solid line is the simulation forced by the unperturbed SAFRAN analysis. The blue patterns represent the envelopes including the 300 members which are shown by the black lines.

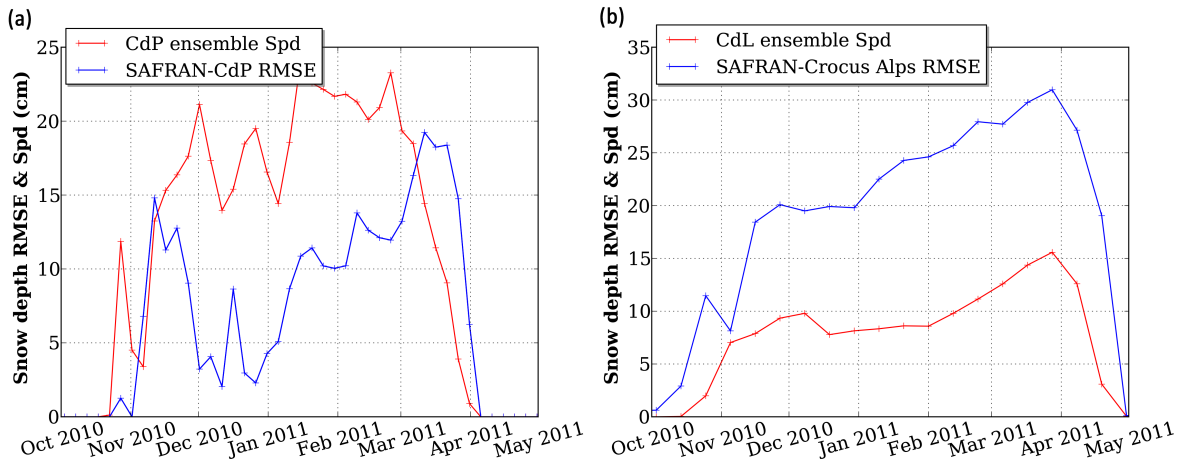


Figure 2. Time evolution over the 2010/2011 season of (in red) the SD ensemble Spd with respect to the ensemble mean and (in blue) the SD RMSE between SAFRAN-Crocus estimates and *in-situ* observations. (a) for the CdP site and (b) for the CdL ensemble compared to the multiple Alps stations at the same elevation than CdL.

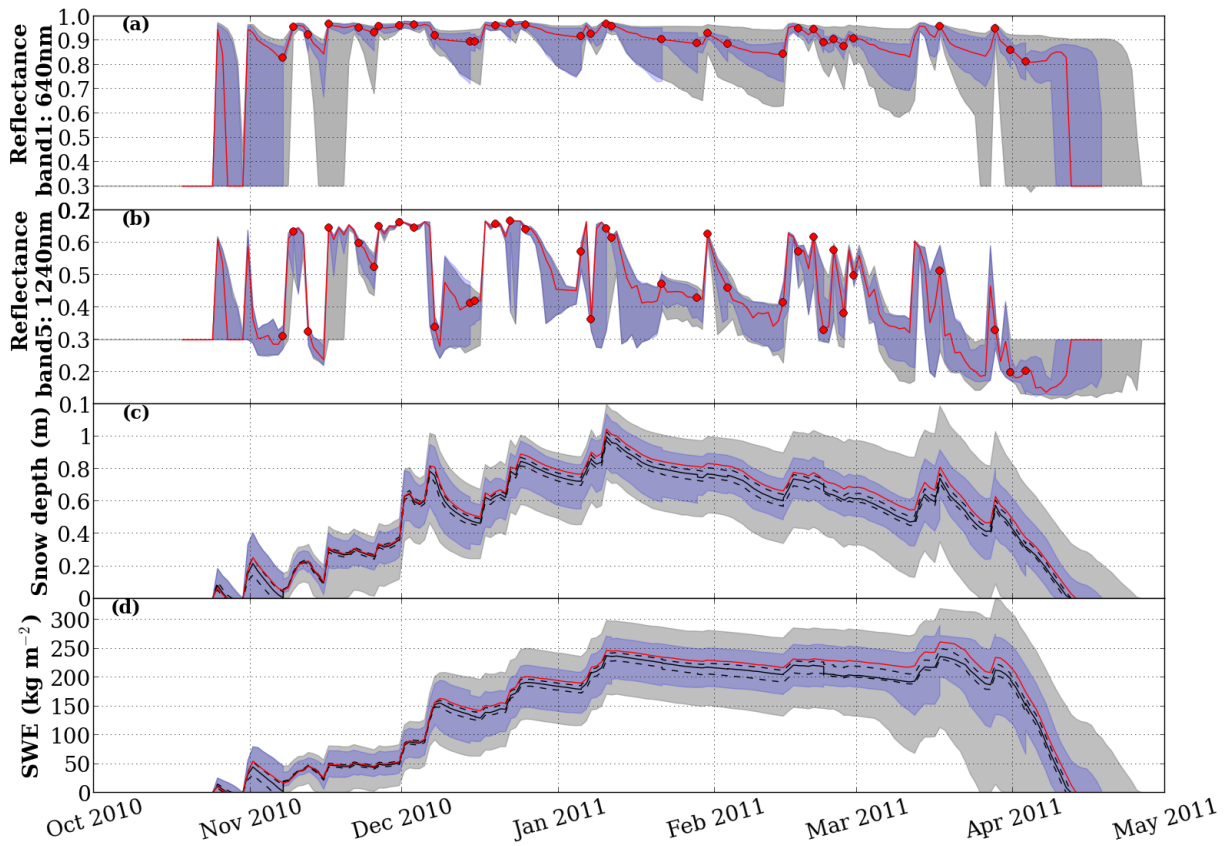


Figure 3. Evolution of the ensemble over the 2010/2011 season. (a) and (b) Reflectance at 640 nm and 1240 nm (first and fifth MODIS band, respectively), (c) SD and (d) SWE. The blue shading represent the envelopes of the ensemble assimilating MODIS-like reflectances and the grey patterns the envelopes of the ensemble without assimilation. The red lines represent the control simulation (synthetic truth). On graph (a) and (b), the red dots show the assimilated observations. On both (c) and (d), the black solid line shows the 50% quantiles (median of the ensemble) and the black dotted lines the 33% and 67% quantiles for the baseline experiment.

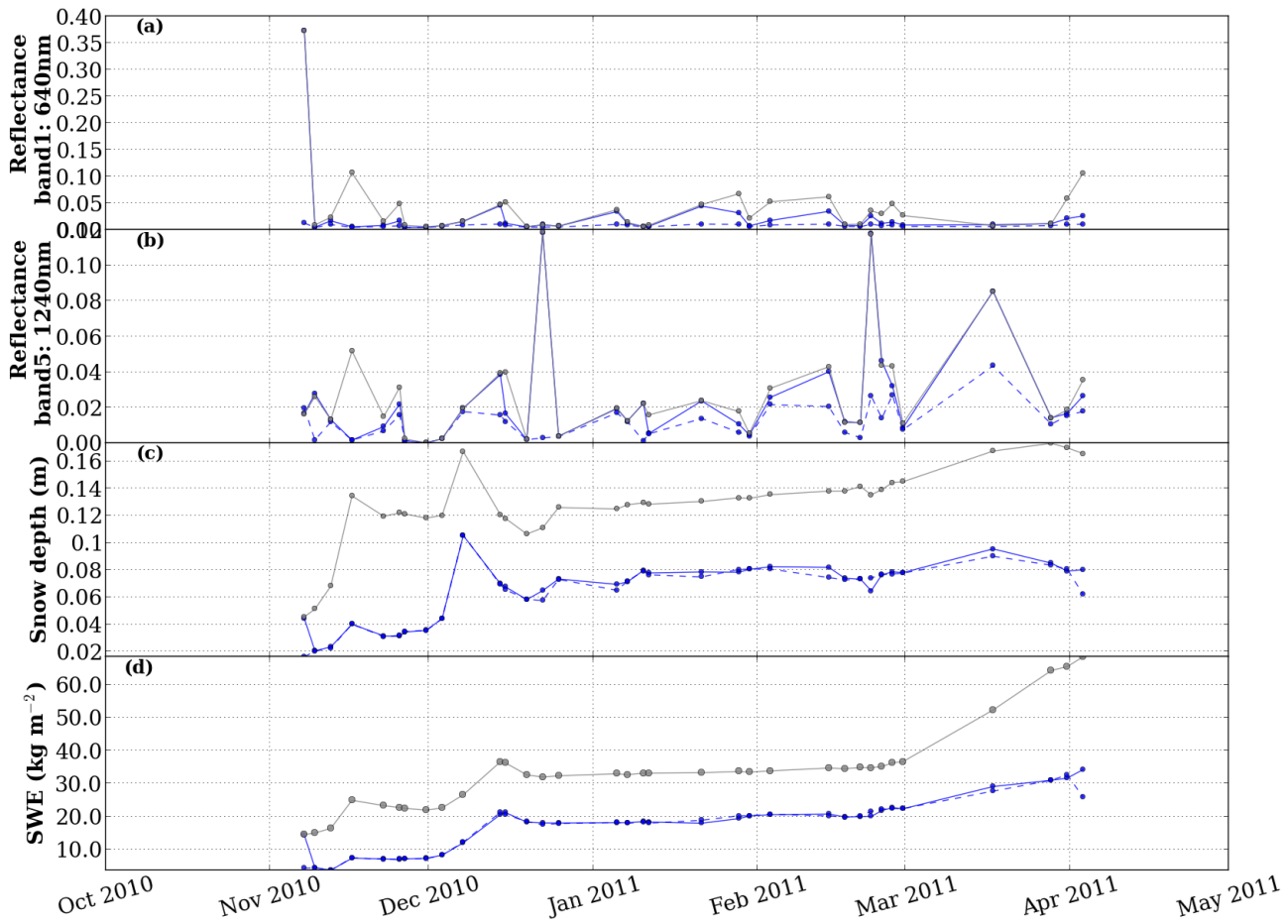


Figure 4. Time evolution of the ensemble RMSEs on (a) Reflectance at 640 nm, (b) reflectance at 1240 nm, (c) SD and (d) SWE, over the 2010/2011 season, for the run without assimilation (grey lines), and the baseline assimilation experiment (Blue solid line: forecast; blue dotted line: analysis). Dots indicate analysis steps.

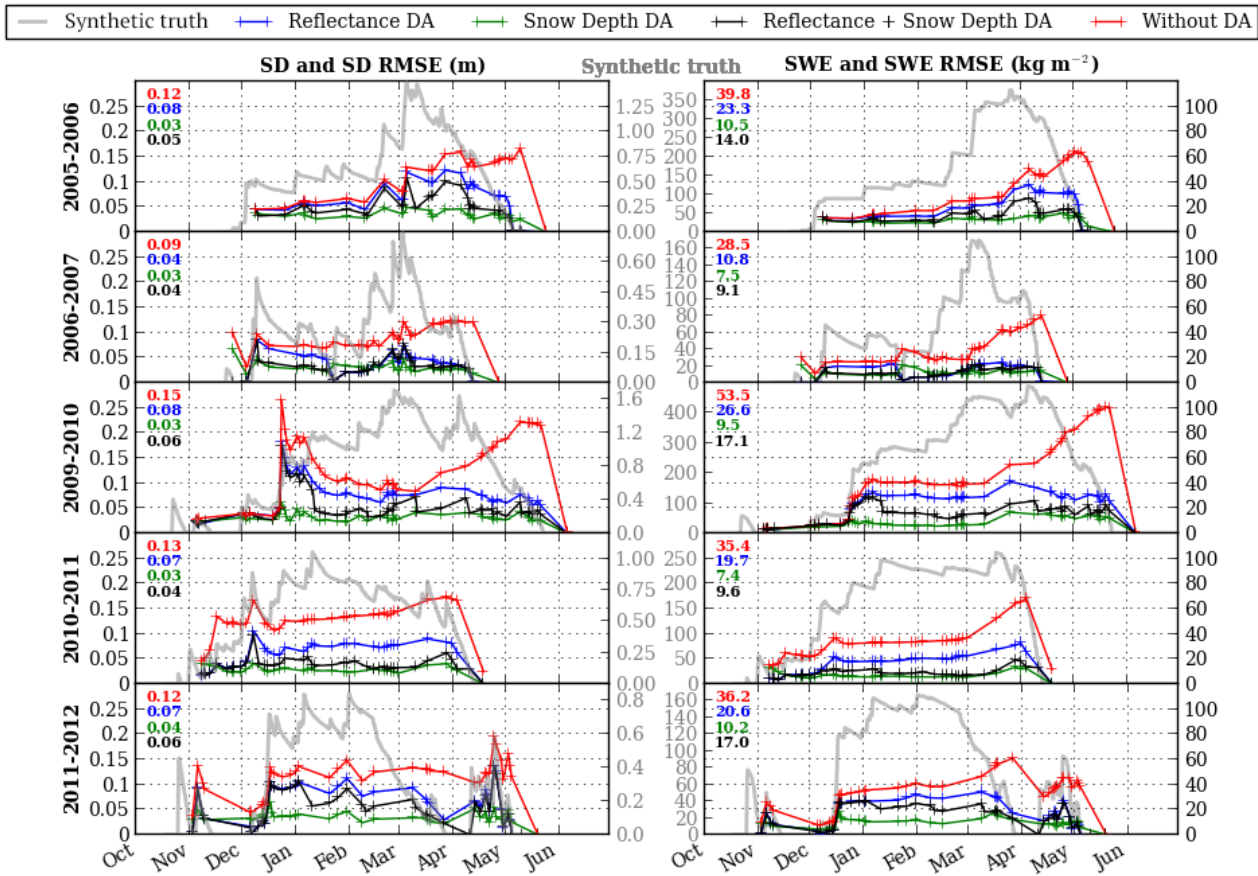


Figure 5. Time evolution of ensemble RMSEs on SD (left) and SWE (right) for the five seasons under study, for the run without assimilation (red lines), the baseline experiment (assimilating reflectances, blue lines), the experiment assimilating SD data (green lines) and the experiment assimilating combined reflectances and SD data (black lines). Crosses indicate analysis steps. **Seasonal averages** are displayed in the upper left corner of each graph. The model control simulation is represented by the grey lines, scaled by the "Synthetic truth" y-axes.

TABLES:

Variables	CdP: Reanalysis - Observations		CdL: Reanalysis - Ensemble	
	Bias	std: σ_{CdP}	Bias	std: σ_{CdL}
Air temperature (C)	0.28	1.08	5.0 e-03	1.07
Wind speed (m s^{-1})	0.2	1.12 (0.6)	4.0 e-04	0.4
Shortwave radiation (W m^{-2})	22.4	79 (70)	-3.1 e-03	58.3
Longwave radiation (W m^{-2})	-14.0	24.5 (7)	2.0 e-02	7.0
Snowfall rate ($\text{kg m}^{-2} \text{h}^{-1}$)	-2.0 e-02	0.4	5.0 e-03	0.1
Rainfall rate ($\text{kg m}^{-2} \text{h}^{-1}$)	7.2 e-03	0.5	-5.0 e-03	0.1

Table 1. Bias and standard deviations (std) of the differences between SAFRAN reanalysis and *in-situ* observations (left) and the differences between SAFRAN reanalysis and the ensemble built up in the present study (right), for the perturbed meteorological forcings. The first set of statistics is derived from 18 years (**1993-2011**) of observations and reanalysis at the CdP and the second set is derived from our 300-members ensemble over the 2010/2011 hydrological season. **The values in brackets correspond to the adjusted standard deviation used to generate the ensemble at CdL site.**

Results reported in	Fig. 1	Fig. 3	Fig. S7	Fig. S2	Fig. S3	Fig. S4	Fig. S5	Fig. S6	Fig. S8	Fig. 5
Variable assimilated	No AD	Baseline Refl.	SD	Clear sky days	All days Refl.	Melt Refl.	Before Snowf Refl.	After Snowf Refl.	Refl. + SD	Refl.
Assimilation timing	No AD	Baseline	Clear sky days	All days	Accu.	Melt	Before Snowf	After Snowf	All seasons	All seasons
SD (m)	0.13	0.07	0.03	0.05	0.05	0.12	0.07	0.12	0.04	0.07
SWE (kg m^{-2})	35.4	19.7	7.4	14.4	12.9	35.5	21.8	37.2	9.6	20.2

Table 2. SD and SWE seasonal averaged RMSE computed with respect to the synthetic truth for all experiments over the 2010/2011 season. Results reported in Fig. 5 are the RMSE computed over the 5 selected seasons.

References

- Abaza, M., Anctil, F., Fortin, V., and Turcotte, R.: Exploration of sequential streamflow assimilation in snow dominated watersheds, *Advances in Water Resources*, 80, 79–89, 2015.
- 755 Andreadis, K. M. and Lettenmaier, D. P.: Assimilating remotely sensed snow observations into a macroscale hydrology model, *Advances in Water Resources*, 29, 872–886, doi:10.1016/j.advwatres.2005.08.004, 2006.
- Bartelt, P. and Lehning, M.: A physical SNOWPACK model for the Swiss avalanche warning: Part I: numerical model, *Cold Regions Science and Technology*, 35, 123–145, doi:10.1016/S0165-232X(02)00074-5, 2002.
- Bavay, M., Grünewald, T., and Lehning, M.: Response of snow cover and runoff to climate
760 change in high Alpine catchments of Eastern Switzerland, *Advances in water resources*, 55, 4–16, doi:10.1016/j.advwatres.2012.12.009, 2013.
- Blayo, É., Bocquet, M., Cosme, E., and Cugliandolo, L. F.: *Advanced Data Assimilation for Geosciences: Lecture Notes of the Les Houches School of Physics: Special Issue, June 2012*, Oxford University Press, 2014.
- 765 Boone, A. and Etchevers, P.: An intercomparison of three snow schemes of varying complexity coupled to the same land surface model: Local-scale evaluation at an Alpine site, *Journal of Hydrometeorology*, 2, 374–394, doi:http://dx.doi.org/10.1175/1525-7541(2001)002<0374:AIOTSS>2.0.CO;2, 2001.
- Brun, E., Martin, E., Simon, V., Gendre, C., and Coléou, C.: An energy and mass model of snow cover suitable for operational avalanche forecasting, *J. Glaciol.*, 35, 333 – 342, 1989.
- 770 Brun, E., David, P., Sudul, M., and Brunot, G.: A numerical model to simulate snow-cover stratigraphy for operational avalanche forecasting, *J. Glaciol.*, 38, 13 – 22, [http://refhub.elsevier.com/S0165-232X\(14\)00138-4/rf0155](http://refhub.elsevier.com/S0165-232X(14)00138-4/rf0155), 1992.
- Brun, F., Dumont, M., Wagnon, P., Berthier, E., Azam, M., Shea, J., Sirguey, P., Rabatel, A., and Ramanathan, A.: Seasonal changes in surface albedo of Himalayan glaciers from MODIS data and links with the annual
775 mass balance, *The Cryosphere*, 9, 341–355, doi:10.5194/tc-9-341-2015, 2015., 2015.
- Bühler, Y., Marty, M., Egli, L., Veitinger, J., Jonas, T., Thee, P., and Ginzler, C.: Snow depth mapping in high-alpine catchments using digital photogrammetry, *The Cryosphere*, 9, 229–243, doi:10.5194/tc-9-229-2015, <http://www.the-cryosphere.net/9/229/2015/>, 2015.
- Carmagnola, C., Morin, S., Lafaysse, M., Domine, F., Lesaffre, B., Lejeune, Y., Picard, G., and Arnaud,
780 L.: Implementation and evaluation of prognostic representations of the optical diameter of snow in the SURFEX/ISBA-Crocus detailed snowpack model, *The Cryosphere*, 8, 417–437, doi:10.5194/tc-8-417-2014, 2014.
- Carpenter, T. M. and Georgakakos, K. P.: Impacts of parametric and radar rainfall uncertainty on the ensemble streamflow simulations of a distributed hydrologic model, *Journal of Hydrology*, 298, 202–221,
785 doi:10.1016/j.jhydrol.2004.03.036, 2004.
- Castebrunet, H., Eckert, N., Giraud, G., Durand, Y., and Morin, S.: Projected changes of snow conditions and avalanche activity in a warming climate: the French Alps over the 2020-2050 and 2070-2100 periods, *Cryosphere*, 8, 1673–1697, doi:10.5194/tc-8-1673-2014, 2014.
- Che, T., Li, X., Jin, R., and Huang, C.: Assimilating passive microwave remote sensing data into a land surface
790 model to improve the estimation of snow depth, *Remote Sensing of Environment*, 143, 54–63, 2014.

- Clark, M. P., Slater, A. G., Barrett, A. P., Hay, L. E., McCabe, G. J., Rajagopalan, B., and Leavesley, G. H.: Assimilation of snow covered area information into hydrologic and land-surface models, *Advances in water resources*, 29, 1209–1221, 2006.
- 795 Cordisco, E., Prigent, C., and Aires, F.: Snow characterization at a global scale with passive microwave satellite observations, *Journal of Geophysical Research: Atmospheres* (1984–2012), 111, doi:10.1029/2005JD006773, 2006.
- De Lannoy, G. J. M., Reichle, R. H., Arsenault, K. R., Houser, P. R., Kumar, S., Verhoest, N. E. C., and Pauwels, V. R. N.: Multiscale assimilation of Advanced Microwave Scanning Radiometer–EOS snow water equivalent and Moderate Resolution Imaging Spectroradiometer snow cover fraction observations in northern Colorado, *Water Resources Research*, 48, doi:10.1029/2011WR010588, <http://dx.doi.org/10.1029/2011WR010588>, w01522, 2012.
- 800 Dechant, C. and Moradkhani, H.: Radiance data assimilation for operational snow and streamflow forecasting, *Advances in Water Resources*, 34, 351–364, doi:10.1016/j.advwatres.2010.12.009, 2011.
- Deodatis, G. and Shinozuka, M.: Auto-regressive model for nonstationary stochastic processes, *Journal of Engineering Mechanics*, 114, 1995–2012, doi:[http://dx.doi.org/10.1061/\(ASCE\)0733-9399\(1988\)114:11\(1995\)](http://dx.doi.org/10.1061/(ASCE)0733-9399(1988)114:11(1995)), 1988.
- 805 Doherty, S. J., Grenfell, T. C., Forsström, S., Hegg, D. L., Brandt, R. E., and Warren, S. G.: Observed vertical redistribution of black carbon and other insoluble light-absorbing particles in melting snow, *Journal of Geophysical Research: Atmospheres*, 118, 5553–5569, doi:10.1002/jgrd.50235, 2013.
- 810 Domine, F., Sparapani, R., Ianniello, A., and Beine, H. J.: The origin of sea salt in snow on Arctic sea ice and in coastal regions, *Atmos. Chem. Phys.*, 4, 2259–2271, 2004.
- Dong, J., Walker, J. P., Houser, P. R., and Sun, C.: Scanning multichannel microwave radiometer snow water equivalent assimilation, *Journal of Geophysical Research: Atmospheres* (1984–2012), 112, doi:10.1029/2006JD007209, 2007.
- 815 Dumont, M., Durand, Y., Arnaud, Y., and Six, D.: Variational assimilation of albedo in a snowpack model and reconstruction of the spatial mass-balance distribution of an alpine glacier, *J. Glaciol.*, 58(207), 151 – 164, doi:10.3189/2012JoG11J163, 2012.
- Dumont, M., Brun, E., Picard, G., Michou, M., Libois, Q., Petit, J., Geyer, M., Morin, S., and Josse, B.: Contribution of light-absorbing impurities in snow to Greenland’s darkening since 2009, *Nature Geoscience*, doi:10.1038/ngeo2180, 2014.
- 820 Durand, M., Kim, E. J., and Margulis, S. A.: Radiance assimilation shows promise for snowpack characterization, *Geophysical Research Letters*, 36, doi:10.1029/2008GL035214, 2009.
- Durand, Y., Brun, E., Mérindol, L., Guyomarc’h, G., Lesaffre, B., and Martin, E.: A meteorological estimation of relevant parameters for snow models, *Ann. Glaciol.*, 18, 65–71, http://www.igsoc.org/annals/18/igs_annals_vol18_year1993_pg65-71.html, 1993.
- 825 Durand, Y., Giraud, G., Brun, E., Mérindol, L., and Martin, E.: A computer-based system simulating snowpack structures as a tool for regional avalanche forecasting, *J. Glaciol.*, 45, 469–484, 1999.
- Essery, R., Morin, S., Lejeune, Y., and Menard, C. B.: A comparison of 1701 snow models using observations from an alpine site, *Advances in water resources*, 55, 131–148, doi:10.1016/j.advwatres.2012.07.013, 2013.

- 830 Etchevers, P., Golaz, C., and Habets, F.: Simulation of the water budget and the river flows of the Rhone basin from 1981 to 1994, *Journal of hydrology*, 244, 60–85, doi:10.1016/S0022-1694(01)00332-8, 2001.
- Evensen, G.: *Data assimilation: the ensemble Kalman filter*, Springer Science & Business Media, Berlin, 2009.
- Fortin, V., Abaza, M., Anctil, F., and Turcotte, R.: Why should ensemble spread match the RMSE of the ensemble mean?, *Journal of Hydrometeorology*, 15, 1708–1713, doi:http://dx.doi.org/10.1175/JHM-D-14-0008.1, 835 2014.
- Foster, J. L., Sun, C., Walker, J. P., Kelly, R., Chang, A., Dong, J., and Powell, H.: Quantifying the uncertainty in passive microwave snow water equivalent observations, *Remote Sensing of environment*, 94, 187–203, doi:10.1016/j.rse.2004.09.012, 2005.
- Gabbi, J., Huss, M., Bauder, A., Cao, F., and Schwikowski, M.: The impact of Saharan dust and black carbon 840 on albedo and long-term glacier mass balance, *The Cryosphere Discussions*, 9, 1133–1175, doi:10.5194/tc-9-1385-2015, 2015.
- Gordon, N. J., Salmond, D. J., and Smith, A. F.: Novel approach to nonlinear/non-Gaussian Bayesian state estimation, in: *IEE Proceedings F (Radar and Signal Processing)*, vol. 140, pp. 107–113, IET, 1993.
- Hall, D. K. and Riggs, G. A.: Accuracy assessment of the MODIS snow products, *Hydrol. Process.*, 21, 1534– 845 1547, doi:10.1002/hyp.6715, 2007.
- Jordan, R.: *A One-Dimensional Temperature Model for a Snow Cover: Technical Documentation for SNTHERM*. 89., Tech. rep., Cold Regions Research and Engineering Lab. Hanover NH, 1991.
- Kitagawa, G.: Monte Carlo filter and smoother for non-Gaussian nonlinear state space models, *Journal of computational and graphical statistics*, 5, 1–25, 1996.
- 850 Lehning, M., Völksch, I., Gustafsson, D., Nguyen, T. A., Stähli, M., and Zappa, M.: ALPINE3D: a detailed model of mountain surface processes and its application to snow hydrology, *Hydrological Processes*, 20, 2111–2128, doi:10.1002/hyp.6204, 2006.
- Li, W., Stamnes, K., Chen, B., and Xiong, X.: Snow grain size retrieved from near-infrared radiances at multiple wavelengths, *Geophysical Research Letters*, 28, 1699–1702, doi:10.1029/2000GL011641, 2001.
- 855 Libois, Q., Picard, G., France, J., Arnaud, L., Dumont, M., Carmagnola, C., and King, M.: Influence of grain shape on light penetration in snow, *The Cryosphere*, 7, 1803–1818, doi:10.5194/tc-7-1803-2013, 2013.
- Libois, Q., Picard, G., Dumont, M., Arnaud, L., Sergeant, C., Pougatch, E., Sudul, M., and Vial, D.: Experimental determination of the absorption enhancement parameter of snow, *Journal of Glaciology*, 60, 714–724, doi:10.1002/2014JD022361, 2014.
- 860 Liu, Y., Peters-Lidard, C. D., Kumar, S., Foster, J. L., Shaw, M., Tian, Y., and Fall, G. M.: Assimilating satellite-based snow depth and snow cover products for improving snow predictions in Alaska, *Advances in Water Resources*, 54, 208–227, doi:10.1016/j.advwatres.2013.02.005, 2013.
- López-Moreno, J. I., Fassnacht, S. R., Beguería, S., and Latron, J. B. P.: Variability of snow depth at the plot scale: implications for mean depth estimation and sampling strategies, *The Cryosphere*, 5, 617–629, 865 doi:10.5194/tc-5-617-2011, <http://www.the-cryosphere.net/5/617/2011/>, 2011.
- Masson, V., Le Moigne, P., Martin, E., Faroux, S., Alias, A., Alkama, R., Belamari, S., Barbu, A., Boone, A., Bouyssel, F., Brousseau, P., Brun, E., Calvet, J.-C., Carrer, D., Decharme, B., Delire, C., Donier, S., Essaouini, K., Gibelin, A.-L., Giordani, H., Habets, F., Jidane, M., Kerdraon, G., Kourzeneva, E., Lafaysse, M., Lafont, S., Lebeaupin Brossier, C., Lemonsu, A., Mahfouf, J.-F., Marguinaud, P., Mokhtari, M., Morin,

- 870 S., Pigeon, G., Salgado, R., Seity, Y., Taillefer, F., Tanguy, G., Tulet, P., Vincendon, B., Vionnet, V., and
Voldoire, A.: The SURFEXv7.2 land and ocean surface platform for coupled or offline simulation of earth
surface variables and fluxes, *Geoscientific Model Development*, 6, 929–960, doi:10.5194/gmd-6-929-2013,
<http://www.geosci-model-dev.net/6/929/2013/>, 2013.
- Morin, S.: Observation and numerical modeling of snow on the ground : use of existing tools and contribution
875 to ongoing developments, *Habilitation à diriger des recherches*, Université Joseph Fourier, Grenoble, <https://tel.archives-ouvertes.fr/tel-01098576>, 2014.
- Morin, S., Lejeune, Y., Lesaffre, B., Panel, J.-M., Poncet, D., David, P., and Sudul, M.: A 18-years long (1993 -
2011) snow and meteorological dataset from a mid-altitude mountain site (Col de Porte, France, 1325 m alt.)
for driving and evaluating snowpack models, *Earth Syst. Sci. Data*, 4, 13–21, doi:10.5194/essd-4-13-2012,
880 2012.
- Navari, M., Margulis, S., Bateni, S., Tedesco, M., Alexander, P., and Fettweis, X.: Feasibility of improving
a priori regional climate model estimates of Greenland ice sheet surface mass loss through assimilation of
measured ice surface temperatures, *Cryosphere (The)*, 10, 103–120, 2016.
- Noilhan, J. and Planton, S.: A simple parameterization of land surface processes for meteorological models,
885 *Mon. Weather Rev.*, 117, 536–549, doi:10.1175/1520-0493(1989)117<0536:ASPOLS>2.0.CO;2, 1989.
- Painter, T. H., Barrett, A. P., Landry, C. C., Neff, J. C., Cassidy, M. P., Lawrence, C. R., McBride, K. E., and
Farmer, G. L.: Impact of disturbed desert soils on duration of mountain snow cover, *Geophysical Research
Letters*, 34, n/a–n/a, doi:10.1029/2007GL030284, <http://dx.doi.org/10.1029/2007GL030284>, 112502, 2007.
- Phan, X. V., Ferro-Famil, L., Gay, M., Durand, Y., Dumont, M., Morin, S., Allain, S., D’Urso, G., and Girard,
890 A.: 1D-Var multilayer assimilation of X-band SAR data into a detailed snowpack model, *The Cryosphere*, 8,
1975–1987, doi:10.5194/tc-8-1975-2014, 2014.
- Quintana Segui, P., Moigne, P. L., Durand, Y., Martin, E., Habets, F., Baillon, M., Canella, C., Franchisteguy,
L., and Morel, S.: Analysis of near surface atmospheric variables : validation of the SAFRAN analysis over
France, *J. Appl. Meteor. Climat.*, 47(1), 92–107, doi:10.1175/2007JAMC1636.1, 2008.
- 895 Raleigh, M., Lundquist, J., and Clark, M.: Exploring the impact of forcing error characteristics on physically
based snow simulations within a global sensitivity analysis framework, *Hydrology and Earth System Sci-
ences*, 19, 3153–3179, doi:10.5194/hessd-11-13745-2014, 2015.
- Reichle, R. H.: Data assimilation methods in the Earth sciences, *Advances in Water Resources*, 31, 1411–1418,
2008.
- 900 Sirguey, P., Mathieu, R., and Arnaud, Y.: Subpixel monitoring of the seasonal snow cover with MODIS at 250m
spatial resolution in the Southern Alps of New Zealand: methodology and accuracy assessment, *Remote
Sens. Environ.*, 113, 160–181, doi:10.1016/j.rse.2008.09.008, 2009.
- Snyder, C., Bengtsson, T., Bickel, P., and Anderson, J.: Obstacles to high-dimensional particle filtering, *Monthly
Weather Review*, 136, 4629–4640, doi:10.1175/2008MWR2529.1, 2008.
- 905 Stankov, B., Cline, D., Weber, B., Gasiewski, A., and Wick, G.: High-resolution airborne polarimetric mi-
crowave imaging of snow cover during the NASA cold land processes experiment, *Geoscience and Remote
Sensing, IEEE Transactions on*, 46, 3672–3693, doi:10.1109/TGRS.2008.2000625, 2008.

- Sun, C., Walker, J. P., and Houser, P. R.: A methodology for snow data assimilation in a land surface model, *Journal of Geophysical Research: Atmospheres*, 109, n/a–n/a, doi:10.1029/2003JD003765, <http://dx.doi.org/10.1029/2003JD003765>, d08108, 2004.
- 910 Tedesco, M., Reichle, R., Löw, A., Markus, T., and Foster, J. L.: Dynamic approaches for snow depth retrieval from spaceborne microwave brightness temperature, *Geoscience and Remote Sensing, IEEE Transactions on*, 48, 1955–1967, doi:10.1109/TGRS.2009.2036910, 2010.
- Van Leeuwen, P. J.: Particle filtering in geophysical systems, *Monthly Weather Review*, 137, 4089–4114, doi:<http://dx.doi.org/10.1175/2009MWR2835.1>, 2009.
- 915 Van Leeuwen, P. J.: Particle filters for the geosciences, *Advanced Data Assimilation for Geosciences: Lecture Notes of the Les Houches School of Physics: Special Issue, June 2012*, p. 291, doi:10.1093/acprof:oso/9780198723844.003.0013, 2014.
- Veitinger, J., Sovilla, B., and Purves, R. S.: Influence of snow depth distribution on surface roughness in alpine terrain: a multi-scale approach, *The Cryosphere*, 8, 547–569, doi:10.5194/tc-8-547-2014, <http://www.the-cryosphere.net/8/547/2014/>, 2014.
- 920 Vernay, M., Lafaysse, M., Mérindol, L., Giraud, G., and Morin, S.: Ensemble forecasting of snowpack conditions and avalanche hazard, *Cold Regions Science and Technology*, doi:10.1016/j.coldregions.2015.04.010, 2015.
- 925 Vionnet, V., Brun, E., Morin, S., Boone, A., Martin, E., Faroux, S., Moigne, P. L., and Willemet, J.-M.: The detailed snowpack scheme Crocus and its implementation in SURFEX v7.2, *Geosci. Model. Dev.*, 5, 773–791, doi:10.5194/gmd-5-773-2012, 2012.
- Warren, S.: Optical properties of snow, *Rev. Geophys.*, 20, 67–89, doi:10.1029/RG020i001p00067, 1982.
- Warren, S. G. and Clarke, A. D.: Soot in the atmosphere and snow surface of Antarctica, *Journal of Geophysical Research: Atmospheres (1984–2012)*, 95, 1811–1816, doi:10.1029/JD095iD02p01811, 1990.
- 930 Wright, P., Bergin, M., Dibb, J., Lefer, B., Domine, F., Carman, T., Carmagnola, C. M., Dumont, M., Courville, Z., Schaaf, C., and Wang, Z.: Comparing MODIS daily snow albedo to spectral albedo field measurements in Central Greenland, *Remote Sensing of Environment*, 140, 118–129, doi:10.1016/j.rse.2013.08.044, 2014.